

# IoT Firmware Version Identification Using Transfer Learning with Twin Neural Networks

ASHLEY ANDREWS, University of Bristol, United Kingdom

GEORGE OIKONOMOU, University of Bristol, United Kingdom

SIMON ARMOUR, University of Bristol, United Kingdom

PAUL THOMAS, University of Bristol, United Kingdom

THOMAS CATTERMOLLE, Tiberos Research, United Kingdom

As the Internet of Things (IoT) becomes more embedded within our daily lives, there is growing concern about the risk ‘smart’ devices pose to network security. To address this, one avenue of research has focused on automated IoT device identification. This research is broadly motivated by the idea that the more we can know about our devices, the more secure the networks they are on can be. Research has however largely neglected the identification of IoT device firmware versions. There is strong evidence that IoT security relies on devices being on the latest version patched for known vulnerabilities. Identifying when a device has updated (has changed version) or not (is on a stable version) is therefore useful for IoT security. Version identification involves challenges beyond those for identifying the model, type, and manufacturer of IoT devices. Most obviously, the differences between versions are more subtle and therefore harder to detect. Moreover, because there has been relatively little research in this area, there are no widely available datasets that track devices’ version changes over time. Consequently, traditional machine learning algorithms are ill-suited for effective version identification due to being limited by the availability of data for training. In this paper, we introduce an effective technique for identifying IoT device versions based on transfer learning. This technique relies on the idea that we can use a Twin Neural Network (TNN) – trained at distinguishing devices – to detect differences between a device on different versions. This facilitates real-world implementation by requiring relatively little training data. In more detail, we extract statistical features from on-wire packet flows, convert these features into greyscale images, pass these images into a TNN to output similarity scores, and determine version changes based on the Hedges’  $g$  effect size of the similarity scores. This allows us to detect the subtle changes present in on-wire traffic when a device changes version. To evaluate our technique, we set up a lab containing 12 IoT devices and recorded their on-wire packet captures for 11 days across multiple firmware versions. For testing data held out from training, our best performing model is shown to be 95.83% and 84.38% accurate at identifying stable versions and version changes respectively.

CCS Concepts: • **Security and privacy** → **Network security**; • **Computing methodologies** → **Neural networks**.

Additional Key Words and Phrases: Internet of Things (IoT), Device Identification, Twin Neural Networks, Firmware Versions

## ACM Reference Format:

Ashley Andrews, George Oikonomou, Simon Armour, Paul Thomas, and Thomas Cattermole. 2024. IoT Firmware Version Identification Using Transfer Learning with Twin Neural Networks. 1, 1 (January 2024), 30 pages. <https://doi.org/XXXXXXX.XXXXXXX>

Authors’ addresses: Ashley Andrews, University of Bristol, Bristol, United Kingdom, [ash.andrews@bristol.ac.uk](mailto:ash.andrews@bristol.ac.uk); George Oikonomou, University of Bristol, Bristol, United Kingdom, [g.oikonomou@bristol.ac.uk](mailto:g.oikonomou@bristol.ac.uk); Simon Armour, University of Bristol, Bristol, United Kingdom, [simon.armour@bristol.ac.uk](mailto:simon.armour@bristol.ac.uk); Paul Thomas, University of Bristol, Bristol, United Kingdom, [paul.thomas@bristol.ac.uk](mailto:paul.thomas@bristol.ac.uk); Thomas Cattermole, Tiberos Research, London, United Kingdom, [thomas.cattermole@tiberos.co.uk](mailto:thomas.cattermole@tiberos.co.uk).

Permission to make digital or hard copies of all or part of this work for personal or classroom use is granted without fee provided that copies are not made or distributed for profit or commercial advantage and that copies bear this notice and the full citation on the first page. Copyrights for components of this work owned by others than the author(s) must be honored. Abstracting with credit is permitted. To copy otherwise, or republish, to post on servers or to redistribute to lists, requires prior specific permission and/or a fee. Request permissions from [permissions@acm.org](mailto:permissions@acm.org).

© 2024 Copyright held by the owner/author(s). Publication rights licensed to ACM.

Manuscript submitted to ACM

Manuscript submitted to ACM

1

## 1 INTRODUCTION

The impact of the Internet of Things (IoT) is increasingly being felt across all aspects of society: in our homes (so-called ‘smart homes’), businesses (industrial IoT), and the public sector (smart cities). As more IoT devices become embedded within our daily lives, there is a growing fear about the potential risk they pose to security (not to mention privacy and safety). These fears have been realised with “smart doorbells being an ‘easy target for hackers” [8] and seemingly innocuous children’s toys allowing attackers access into networks and subsequently homes [7]. To combat this risk, a body of research is developing devoted to automatically identifying IoT devices and understanding their behaviour. Recent work has largely focused on using supervised Machine Learning (ML) to classify wired (and wireless) network traffic in terms of device models, types and manufacturers. Underlying this work is the broad motivation that the more we can know about our IoT devices automatically, the more we can secure the IoT. More specific motivations include: automatically detecting when a rogue device enters a network and automatically detecting when a known device is behaving anomalously and therefore might be compromised.

To fully identify an IoT device, there are four properties as defined by Meidan et al [25]. These are: 1) Type, 2) Manufacturer, 3) Model Number and 4) Firmware Version. IoT device identification down to a software/firmware version level, specifically ensuring a device is running their latest version patched for known vulnerabilities [6], is a motivation that has been largely neglected [4, 5]. In order to be competitive, device manufacturers need to continuously release new products with short time-to-market and lowest possible prices. To this end, in this specific market, it is extremely hard to produce devices with strong security guarantees [12] and therefore flaws and vulnerabilities in devices are prevalent. A recent case with a flaw in Hikvision cameras allowed remote access [9], showing the importance of applying firmware updates to keep devices secure. However even with a serious vulnerability and a patch available, a whitepaper published 12 months later by Cyfirma [14] showed the patches had not been applied to over 80,000 internet reachable devices. This neglected motivation therefore has a concrete real-world application for IoT security: if we can automate version identification we can keep IoT devices up to date without user intervention, reducing their burden.

Version identification is however a more difficult problem to solve than other types of identification, such as device type or model. This is because the on-wire changes between versions are expected to be subtle and datasets are not publicly available containing version change information to train ML models. A method needs to be developed that can overcome these two challenges. This paper’s contributions include:

- A technique using transfer learning to identify device version changes without a need to train on a large amount of data, or having seen the data previously. More specifically using the output similarity scores from Twin Neural Networks with Hedges’ g to identify both stable device versions and subtle device version changes,
- Obtaining a best accuracy of 95.83% identifying stable versions and 84.38% identifying version changes on a real world test-bed when using Hedges’ g to identify subtleties on the Twin Neural Network output. The use of Hedges’ g gives an improvement of approximately 20% over alternative metrics,
- A analysis of the difficulties in identifying IoT device firmware version changes seen in our testbed, specifically the subtle differences in on-wire signatures or in some cases no changes at all.

Our structure for the paper is as follows. In Section 2 we give a clear real-world motivation for how automated version identification can improve IoT security. We also describe the challenges of version identification and outline a method for addressing these challenges. In Section 3 we examine the literature around IoT device identification and twin neural networks, including how we can interpret the output similarity scores when applied to IoT device versions. In Section 4 we then use this knowledge for our proposed method, extracting our chosen features to generate pairs

to train and then test the TNN on two scenarios - identification of devices with a stable version and identification of device version changes - using four measures of accuracy. In Section 5 we briefly state the results from training the TNN and for our two test cases. We then complete a more in-depth analysis of the results with limitations of our approach, including analysis of which devices do and do not perform well. We state how these results relate to real-world use in Section 6. In Section 7 we conclude, outlining how our proposal can lead to future work in IoT device identification.

## 2 MOTIVATION

To understand precisely how automatic version identification can help reduce the security burden in the IoT, it is worth considering what is demanded of users without automation. Without automation, a user must perform two preliminary administrative tasks for each IoT device to ensure it is up to date (see left side of Fig. 1):

- (1) Find the latest version available for their IoT device.
- (2) Find the current versions that their IoT device is using.

The user is then tasked with comparing the results of (1) and (2): if the current version is not the latest version available, the user should update the device; if they are the same, the user should do nothing. Task (1) typically involves navigating to the relevant manufacturer website for the IoT device in question and checking the latest release notes. Task (2) typically involves accessing the IoT device's designated app and looking at the device's details. Both of these tasks are time-consuming, and it is impractical to heavily rely on manual operations when securing a large number of IoT devices [40]. (2) is typically more time consuming than (1) because (1) can be done somewhat centrally (e.g. within one browser), while (2) may require accessing and navigating many different apps. Moreover, because navigating a website is more programmatic (e.g. via web-scraping) than accessing and navigating an app, (1) is currently more amenable to automation. Automated version identification (see right side of Fig. 1) removes the need to check the device app and requires checking the manufacturer website only when a device changes its behaviour. Automated version identification also makes it possible to detect compromises, when a device has not updated but is behaving anomalously. Both manual and automated approaches are cyclical throughout the lifetime of the device.

Our proposal rests on the idea that automated version identification can reduce the security burden on users by minimising the time they spend performing (2). In particular, by using ML to continuously detect changes in device behaviour, users do not need to manually access their devices' apps. This is a significant reduction in burden for the user. The security burden can therefore be front-loaded to the device, and at a moment when the administrative burden of the user is also present. Just as a user wants to set up their device only once, we believe that a user should set up their device in terms of security only once. Our solution provides that. Additionally, automated version identification can help users to detect compromises, because when a device is up to date but is behaving anomalously, a system could alert the user that the device should be checked manually.

Automated IoT version identification however is a hard problem to solve in practice. IoT device identification has mainly been looked at as a classification problem where a technique involves training an ML model on known devices and seeing if it is possible to classify other devices of the same class. There are a few issues with this approach however. Firstly a classifier is only as good as the dataset used and although public datasets exist for use with ML techniques ([13, 24, 29, 32]) these datasets do not document initial version information or version changes over time. As devices change versions, the on-wire fingerprint can change and therefore the initial fingerprint may not still be relevant, as shown by Sivanathan et al [31]. Second, even with a dataset available for a ML model, there are a plethora of different devices and versions and so it is not feasible to be able to train a classifier on all possible combinations of data. To

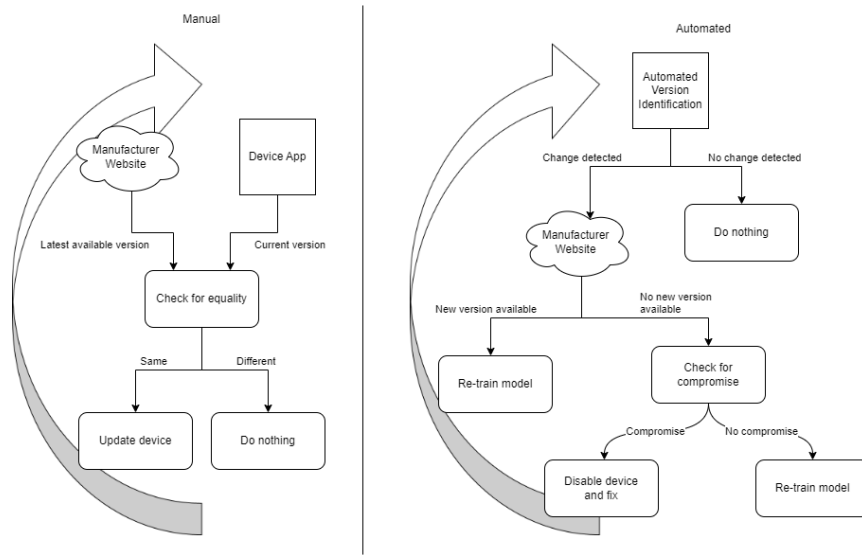


Fig. 1. Comparison between manual and automated management of device versions in the IoT.

overcome the data problem, we can use transfer learning on an initial dataset with a ML approach that outputs similarity scores, such as a twin neural network. This allows us to re-use a pre-trained ML model on a future problem. A similarity based approach has an advantage over a classifier - classification algorithms seem ill-suited to the problem of devices running different versions, as typically a device's fingerprint will remain closer to its original classification than it will to other devices in the model's training set and be erroneously classified. A similarity approach however can state when a device no longer looks similar within a threshold, indicating something has changed.

### 3 BACKGROUND AND PREVIOUS WORK

#### 3.1 IoT Device Identification and Flow-based Features

IoT device identification has been the focus of many studies with various different techniques employed. Techniques include: 1) Rule-based approaches: Creating rules based on a previous understanding of how a device behaves, 2) Unsupervised ML approaches: Using ML techniques to try and find patterns within the data with no prior training phase, 3) Supervised ML: Training and testing an ML model on known labelled data. For any technique the input data is network packets which can be obtained from either: 1) Active methods: Probing a device to elicit a response, or 2) Passive methods: Listening for packets that a device sends without external stimulation. In our study we only consider passive methods, as active methods could interfere with a device and cause it to malfunction. From this data, a common class of features known as 'flow-based features' can be created which have been employed in various studies [3, 24, 27, 31, 32, 37] and therefore is a tangible research angle to pursue. A flow is a succession of packets between a source and a destination characterized by the 4-tuplet (source IP, destination IP, source port, destination port) [1, 3]. These flows can have statistics calculated on them such as the maximum, minimum and average packet size. As well as packet size statistics, packet timing statistics can also be calculated. Some examples include the maximum, minimum and average time between packets that a device sends. Flows can be calculated across different protocols

including NTP [3, 31, 32], DNS [31], discovery protocols such as SSDP or mDNS [3, 23], and also encrypted protocols such as TLS [27]. From analysing flows per protocols for each device, Sivanathan et al. [31] showed that there are "signalling patterns" for protocols meaning devices do the same thing periodically, across different time periods [23], and this periodic communication is different per device [29].

### 3.2 Image-based Classification and Twin Neural Networks

Flow-based features across protocols can be fed into ML algorithms in various ways, including feeding in as a single feature vector, or transforming them first. One common transformation is to convert flow-based features into greyscale images. These techniques work by taking the chosen feature values and parsing them so that they can then be used as gradients of colour values between black (0) and white (255). Although not using the statistics but using the protocol payload data per flow for a varying number of packets, Lim et al. [22] and Xue et al. [39] generate greyscale images from network protocols (as opposed to network data from devices) in an attempt to classify the protocols, similar to Pathmaperuma et al. [28] who use the same technique for user activity detection. Kotak et al. [21] has a similar approach, but applied to IoT device identification. Converting network traffic to greyscale images also has uses within intrusion detection for identifying devices acting maliciously [1, 16, 33] or being part of a botnet [18].

These generated images can then be fed into various neural networks. Neural networks have shown to have use for network security including IoT device identification [34] and intrusion detection [19]. One such neural network is a twin neural network. Introduced by Bromley et al. [11], A Twin (also previously referred to as Siamese) Neural Network, henceforth referred to as a TNN, consists of two identical sub-networks (same architecture, parameters and weights) joined at their outputs. Each sub-network outputs an encoding as a vector, and the two vectors are then compared using a distance metric such as Euclidean distance. This output is then fed into a sigmoid function, such as contrastive loss, which allows a similarity score to be computed, stating how similar the two inputs are. The two metrics that a TNN outputs are accuracy and loss. Accuracy is how well the TNN is able to correctly determine if two input images are the same or not, and loss is a measure of how confident the model is about a prediction. If the images are determined to be the same, the TNN should output a value close to 0 and if they are different the TNN should output a value close to 1, with the threshold being 0.5. TNNs are trained on positive and negative pairs. Positive pairs are pairs that belong to the same class and negative pairs are pairs that belong to different classes. One of the main benefits of using a TNN is that it only requires a small amount of training data to produce accurate results and is also robust to class imbalance. TNNs have also been proposed as a method to solve the ML model retraining problem applied to IoT device identification [35].

Although TNNs are mainly used for image recognition [20] or signature verification [15] they can also be used for network security including intrusion detection [10]. Hindy et al. [17] propose a system to detect network attacks using TNNs, with accuracy across test datasets between 84 and 91%. The main benefits stated by the authors are that the TNN can learn from few instances, lessening the burden of collecting large amounts of data and labelling it. The TNN also allows a single model to be trained which in theory should then be able to classify new, unseen attacks. The main limitations of TNNs is that there needs to be an understanding of how to generate the most useful pairs to train the model - generating every possible combination is not feasible. There also needs to be an architecture for the TNN that is suitable for any future input data.

### 3.3 Statistical Analysis of TNN Output Similarity Scores Using Hedges' g

Similarity score comparison for IoT device identification and determining the threshold for this comparison is an area that needs careful thought. Charyyev et al. [13] use similarity scores with locality-sensitive hashes per device, stating

“One may employ a device-specific threshold based on the variance of the signatures of the device”. One approach that can be used on a per device basis instead of a fixed threshold is Hedges’  $g$ . Hedges’  $g$  is a measure of the difference in means between datasets, and takes into account variability in datasets using the pooled standard deviation [38]. It is defined as:

$$\text{Hedges' } g = \frac{\bar{x}_1 - \bar{x}_2}{s_p} \cdot J \text{ where } s_p = \sqrt{\frac{(n_1 - 1) \cdot S_1^2 + (n_2 - 1) \cdot S_2^2}{n_1 + n_2 - 2}} \text{ and where } J = \left(1 - \frac{3}{4(n_1 + n_2) - 9}\right)$$

And where:

$\bar{x}_1$  and  $\bar{x}_2$  are the means of groups 1 and 2 respectively

$n_1$  and  $n_2$  are the number of samples in groups 1 and 2 respectively

$S_1$  and  $S_2$  are the standard deviations of groups 1 and 2 respectively

$s_p$  is the pooled standard deviation

$J$  is the bias correction factor

What the use of Hedges’  $g$  allows in the context of this paper is to remove the need to apply a fixed similarity threshold for all devices, instead indicating if a significant difference is detected between sample scores for a device. This facilitates generality to different sets of devices. The Hedges’  $g$  score is interpreted in the following way:

- A positive Hedges’  $g$  value indicates that the first group has a larger mean than the second group.
- A negative Hedges’  $g$  value suggests that the second group has a larger mean than the first group.
- The magnitude of the Hedges’  $g$  value provides information about the effect size. Generally, a larger absolute value of  $g$  indicates a stronger effect.

When assessing the practical significance of the effect size ( $g$ ) to decide if it is significant, the following values have been defined by Sawilowsky et al. [30]:

- $|g| \approx 0.01$  - Very Small effect
- $|g| \approx 0.2$  - Small effect
- $|g| \approx 0.5$  - Medium effect
- $|g| \approx 0.8$  - Large effect
- $|g| \approx 1.2$  - Very large effect

It is shown that when a device changes version that the change is normally subtle and harder for a human to notice [4] and so a ‘Medium effect’ is likely to be observed. The differences are much larger [4] between different devices and so it is likely that a ‘Large effect’ is observed.

### 3.4 Application to Our Study

Flow-based features across multiple protocols from IoT network traffic have been shown in this section to be used extensively for IoT device identification, albeit for model identification, not version identification. These features are shown to have periodicity per protocol, and are also shown to be able to be converted into greyscale images suitable for use with neural networks, particularly TNNs, that output a similarity score between two inputs. This shows that

generating greyscale images from network traffic and feeding into a TNN is a feasible approach for IoT device version identification, and using Hedges'  $g$  will allow a technique to identify subtle differences between device versions. We can use this to develop a technique for the following two scenarios applicable to the real world:

**Scenario 1:** Device is on the same version. We would expect the mean similarity score for subsequent days to be within a small threshold from the reference day (but not identical).

**Scenario 2:** Device has updated, therefore there is a subtle change and the Hedges'  $g$  score will show a medium effect.

To understand how this works in practice, we can consider our technique for device version similarity analogous to animal breed similarity (shown in Fig. 2):

- A TNN is trained and validated on similar and dissimilar pairs. In our case, we have different devices each on a single version. This is analogous to different animals each of a single breed.
- For Scenario 1 we want to ensure that our trained TNN can correctly identify the same device on the same version, albeit with slight on-wire differences. This is analogous to being able to identify the same animal and breed but with, for example, a slightly different colour pattern.
- For Scenario 2 we want to ensure that our trained TNN can pick up subtle changes to device versions. This is analogous to identifying subtle differences between different breeds of the same animal.
- Both cases use transfer learning as mentioned in Section 2 - the trained TNN only knows about different devices each on a single version, not different versions per device. This is analogous to the trained TNN knowing about different animals each of a single breed and not different breeds per animal.

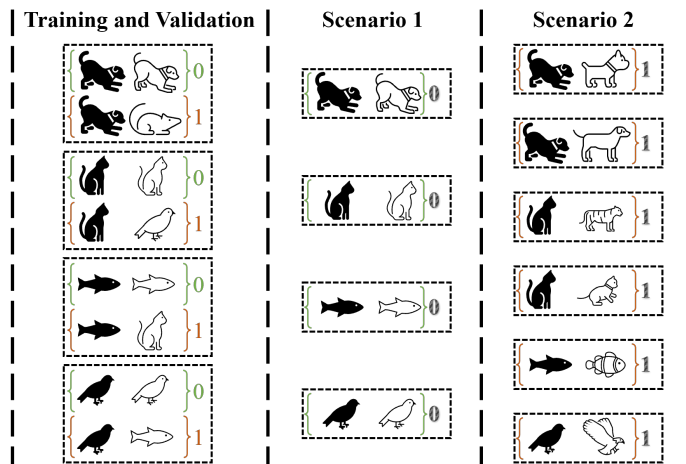


Fig. 2. A visual analogy of our proposed technique as applied to animal classification.

#### 4 METHOD

For our technique, we set ourselves two requirements, based on the Scenarios in Section 3, to be explored in this study:

**Requirement 1:** The technique should reliably identify a device running the same version and not erroneously state there is a difference when there is not,

**Requirement 2:** The technique should be able to correctly identify when a device has changed version.

As mentioned in Section 2, public datasets exist but they do not contain device version information over time, and so to satisfy requirements 1 and 2 we needed to set up our own IoT lab with a traffic capture system to capture all traffic from the IoT devices within the network over time, as they change firmware version. There are an average of 9 devices per UK household [36] and so we set up a lab to mimic a smart home setup with a range of 12 smart devices, connected to a network switch. Our lab devices all generate network traffic and this traffic is mirrored and captured at the switch, called the ‘traffic sniffer’. We use this traffic to train, validate and test our TNN for our two requirements. Our exact methodology around feature selection, image generation, TNN training and testing is covered in the following subsections. This traffic capture system is shown in the top left of Figures 7 and 8 that follow Section 4.4.

#### 4.1 Traffic Analysis and Feature Selection

As shown in Section 3, flow statistics for various protocols can be used for IoT device identification. Based on the literature in Section 3.1, for this study we consider the following protocols: TCP, HTTP, OCSP, TLS, UDP, DNS, NTP, mDNS, SSDP, SIP, QUIC, ICMP and IGMP. There are two types of traffic to use to generate flow statistics per protocol, with advantages and disadvantages to each:

- (1) **Traffic originating from the device only going out of the network** - This has the advantage of not including potential noise from other devices within the local network and is more likely to be applicable across networks. The disadvantage however is that this would not capture anything the device does internally to a network that could be unique, such as pinging a local gateway periodically or setting up a local mesh network.
- (2) **Traffic only between devices locally** - This has the advantage of giving an understanding of how devices interact with each other within a network. This may however only be a small amount of data, or the inter-device communications may not be applicable to other networks containing different device combinations.

We use both (1) and (2), allowing us to use all traffic generated per device potentially giving us the richest data.

When calculating flow statistics for network traffic, there is a decision to make around 1) the time window to create all samples over, i.e. the time window and 2) the sample time to calculate our statistics over, i.e. the time period. For 1), we choose a time window of 6 hours between 00:00 and 06:00 for each device. Our reasoning is as follows: We firstly start our processing at the start of a new day for a device as you’d expect a device to do specific things daily. We would also expect the traffic during this time to be stable and not involve user interaction. 6 hours is also 25% of the data available for a device and so there is a suitable trade-off here between amount of data and processing vs the benefit gained. For 2) we again have a trade-off of processing needs vs benefit. With a smaller sample size, we get more sample points but more processing needs. With a larger sample size, we may not pick up many flow features but less processing power is needed. We also need to consider our sample window boundaries. As shown in Fig. 3 we can see the device clearly has a pattern of 6 packets within the TLS traffic around a potential time window boundary of 00:30, occurring at 00:29:47 and 00:31:47. With a fixed window approach, these packets would be included in two separate sample bins, the first being 00:15:00 - 00:30:00 and the second being 00:30:00 - 00:45:00. We can see however in that same figure, possibly due to network delays or clock drift, these same packets a few days later have shifted, and from this all 6 packets would then appear within the sample bin between 00:30:00 - 00:45:00. Because of this we use a 20% sliding window approach across the network PCAP to capture this temporal information which is sufficient, so in this example our sample bins would be 00:24:00 - 00:39:00, 00:36:00 - 00:51:00 capturing all of the information.



To summarise, we calculate our flow statistics over a time window between 00:00 and 06:00. Within this, we calculate flow statistics over 15 minute windows with a 20% overlap resulting in flow periods 00:00 - 00:15, 00:12 - 00:27, 00:24 - 00:39 etc. giving us 30 datapoints per device per day.

92	00:29:33.616624	192.168.4.127	239.255.255.250	SSDP	606 NOTIFY * HTTP/1.1
93	00:29:33.867136	192.168.4.127	239.255.255.250	SSDP	590 NOTIFY * HTTP/1.1
96	00:30:55.709229	192.168.4.127	ec2-34-242-174-169.eu-we...	TLSv1...	101 Application Data
97	00:30:55.729952	ec2-34-242-174-169.eu-west-1.comp...	192.168.4.127	TLSv1...	97 Application Data
98	00:30:55.730797	192.168.4.127	ec2-34-242-174-169.eu-we...	TCP	66 48302 → 443 [ACK] Seq=141 Ack=125 Win=508
103	00:31:13.993574	192.168.4.127	239.255.255.250	SSDP	743 NOTIFY * HTTP/1.1
104	00:31:13.993730	192.168.4.127	255.255.255.255	SSDP	743 NOTIFY * HTTP/1.1
107	00:32:55.808146	192.168.4.127	ec2-34-242-174-169.eu-we...	TLSv1...	101 Application Data
108	00:32:55.828735	ec2-34-242-174-169.eu-west-1.comp...	192.168.4.127	TLSv1...	97 Application Data
109	00:32:55.830288	192.168.4.127	ec2-34-242-174-169.eu-we...	TCP	66 48302 → 443 [ACK] Seq=176 Ack=156 Win=508
115	00:31:47.729627	192.168.4.127	ec2-34-242-174-169.eu-w...	TLSv1...	101 Application Data
116	00:31:47.769298	ec2-34-242-174-169.eu-west-1.comp...	192.168.4.127	TCP	66 443 → 48302 [ACK] Seq=125 Ack=176 Win=327
117	00:31:48.843922	ec2-34-242-174-169.eu-west-1.comp...	192.168.4.127	TLSv1...	97 Application Data
118	00:31:48.844697	192.168.4.127	ec2-34-242-174-169.eu-w...	TCP	66 48302 → 443 [ACK] Seq=176 Ack=156 Win=508
119	00:31:49.347350	192.168.4.127	no-reverse-defined.uos...	NTP	90 NTP Version 4, client

Fig. 3. Device packets either side of a time window boundary.

## 4.2 Conversion to Greyscale Image

With our flow features extracted, we then create greyscale images per flow period (15 minute sliding window) over 6 hours for use with our TNN. For each device we therefore have a maximum of 30 images per day. There is difficulty in providing a technique that can capture all the information across protocols as one set of features, while still considering how the features can affect each other. This is why our implementation of a greyscale image can work well - it allows patterns both between and within protocols to be noticed. An example image is given in Fig.4. We do the following to create our greyscale images. The Y axis per image is the 13 protocols we have calculated statistics over mentioned in the previous subsection. The X axis becomes the features calculated from the flow statistics, shown in Table 1. For each feature, we normalize the value between 0 and 255 to be suitable for a greyscale image, but group together features for normalization in the following way for 4 different sets of features (shown separated as red dashed lines within Fig. 4):

- The first set are relevant across the protocols, and are normalized *across the protocols*,
- The second set are related to packets and generally large values and are normalised *per protocol*,
- The third set are related to timings and are generally small values and normalised *per protocol*,
- The fourth set are related to ports and will have a standard maximum and minimum value and are normalised *per protocol*.

This then gives an X by Y image per device per sample period with all values between 0 (black) and 255 (white). This gives a fingerprint for a device which can look unique at a high level, and may have more nuanced pixel differences that a TNN can identify. We clean our dataset of input images by removing any images that contain no useful data, i.e. are fully black or white. We can then visualise these images before passing into a TNN. We provide a visualisation with all information in Fig.4, but omit the axis labels in subsequent sections for space saving reasons. Once the greyscale images are created per time period per device, we then need to make pairs to train the TNN.

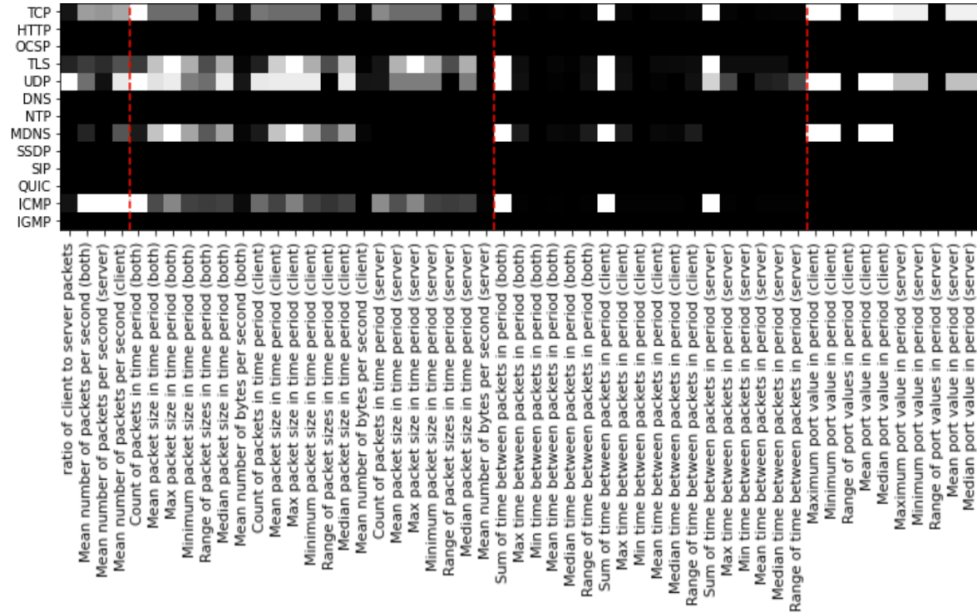


Fig. 4. Example greyscale image, showing protocols on the Y axis and features on the X axis.

Feature Set	For Client (C), Server (S) or Both (B)	Feature Description	Image Section Feature Count
Statistics across all protocols	C   S	Ratio of client to server packets	4
	C   S   B	Mean number of packets per second	
Packet features across each protocol	C   S   B	Count of packets in time period	21
		Mean packet size in time period	
		Max packet size in time period	
		Minimum packet size in time period	
		Range of packet sizes in time period	
		Median packet size in time period	
		Mean number of bytes per second	
		Median number of bytes per second	
Timing features across each protocol	C   S   B	Sum of time between packets in period	18
		Max time between packets in period	
		Min time between packets in period	
		Mean time between packets in period	
		Median time between packets in period	
		Range of time between packets in period	
Port features across each protocol	C   S	Maximum port value in period	10
		Minimum port value in period	
		Range of port values in period	
		Mean port value in period	
		Median port value in period	

Table 1. Features used in greyscale image creation and which section of the image they occupy.

### 4.3 Training the Twin Neural Network

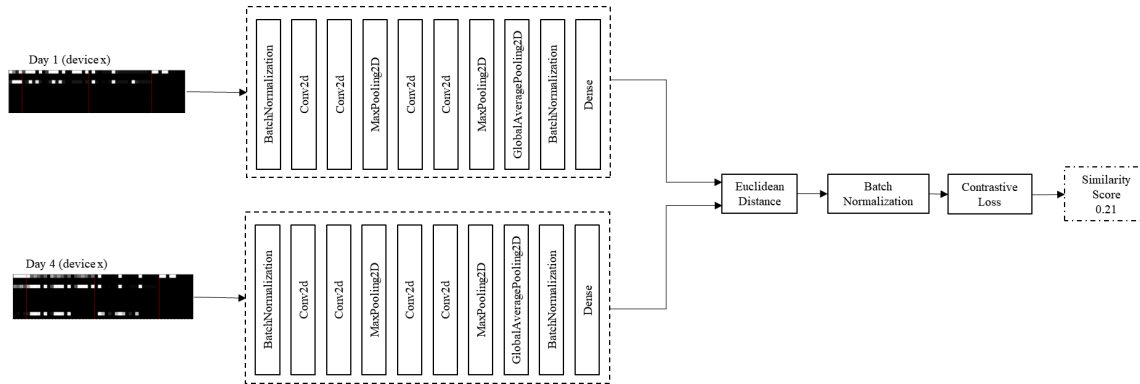


Fig. 5. Internal architecture of our TNN showing the chosen layers with contrastive loss.

Number of Classes	Batch Size	Epochs	Early Stopping	Margin for Contrastive loss
12	50	50	Yes - Validation Loss	1

Table 2. Parameters chosen to create our TNN.

As we are using a *twin* neural network, the architecture of our TNN contains two identical subnetworks, with each arm receiving an input. We feed in two images and get the TNN to produce a similarity score between the two inputs. The architecture with our chosen layers is shown in Fig. 5. Our parameters used when creating our TNN are shown in Table 2. We create positive pairs, pairs where both images belong to the same class, and negative pairs, where the images are from different classes. We ensure our input dataset is balanced, i.e. the number of positive and negative pairs are the same, and the negative pairs are varied across classes by generating pairs in the following way (as shown in Fig. 6):

- (1) **Generating similar pairs for training and validation:** We take each image from **day 1** and pair it to every image for the same device on a single version from **day 2 for training** or **day 3 for validation**.
- (2) **Generating dissimilar pairs for training and validation:** We again take each image from **day 1** and pair it with a random selected image from a randomly selected difference device on a single version from **day 2 for training** or **day 3 for validation**.
- (3) **Generating similar pairs for experiment 1:** For each device, we take each image from **day1** and pair it to every image for the same device on the same version from **days 4-7**.
- (4) **Generating dissimilar pairs for experiment 2:** For each device, we take each image from **day1** and pair it to every image for the same device on the a different version from **days 8-11**.

Using this approach, the maximum number of similar pairs per device, per day is  $30 * 30 = 900$ , and we therefore randomly select the same number of dissimilar pairs. This however is reliant on there being enough data from a device to generate statistics, i.e. some traffic in every 15 minute window. If not, the number of samples, and therefore pairs, will decrease. We generate the pairs in this way for two reasons. First, we use chronological days, which is preferred to

a random split of data [6] and second, we consider the real-world use of our tool being used within a network when training, validating and testing a TNN. A typical deployment would be as follows. Our tool would be deployed and collect network traffic from all devices. The data from day 1 is the baseline day, showing what the network should look like under normal circumstances. We then train and validate our TNN on the training (day 1 and 2) pairs and validation (day 1 and 3) pairs, which allows our TNN to learn what similar device samples look like. We then test on subsequent days paired with day 1.

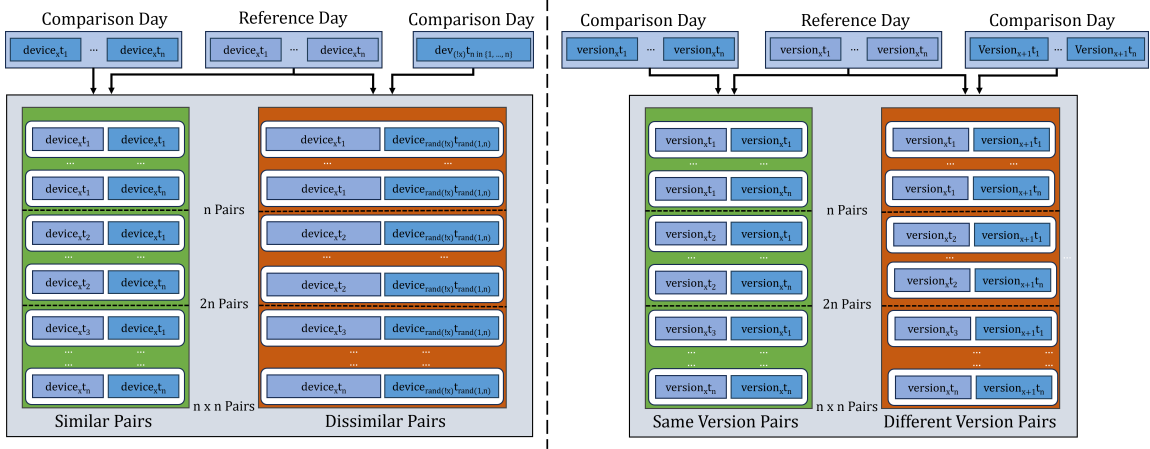


Fig. 6. The creation of pairs for training and validation (left side) and testing (right side) in diagram form. For our study, the number of devices is 12 and the pictorial flow is for all integer values of  $x$  between 1 and 12. We expect  $n$ , the maximum value for the index of the time window, to be 30 in most cases, if all timeslot images exist.

Our full end-to-end system for training our TNN is shown in Fig. 7. Our IoT lab traffic is sniffed to generate PCAP files per device, which then allows feature extraction and image creation (1). Day 1 and 2 data is used to generate the similar and dissimilar training pairs (2), with days 1 and 3 data used to generate the similar and dissimilar validation pairs (3). The TNN is then created using the training and validation pairs, with early stopping monitoring validation loss (4). This then gives us a Trained TNN (5).

#### 4.4 Evaluating the Technique

To evaluate our technique, we will perform the following experiments linking back to our requirements 1 and 2 from Section 4. We will first train our TNN on devices where the versions do not change and ensure that across training and validation we get a good accuracy score and are not overfitting on our data. We will then perform the following two specific experiments using our trained TNN:

**Experiment 1:** We will test our TNN on multiple days of data from each device (where there are no version changes), outputting the overall accuracy per device.

**Experiment 2:** We will test our TNN on multiple days of data from each device where there is a version change. We will again output the overall accuracy per device.

For experiments 1 and 2 we do the following. We feed the pairs into the trained TNN, get the similarity scores for the inputs and use these to produce accuracy scores. For our technique we need a way to quantitatively measure the

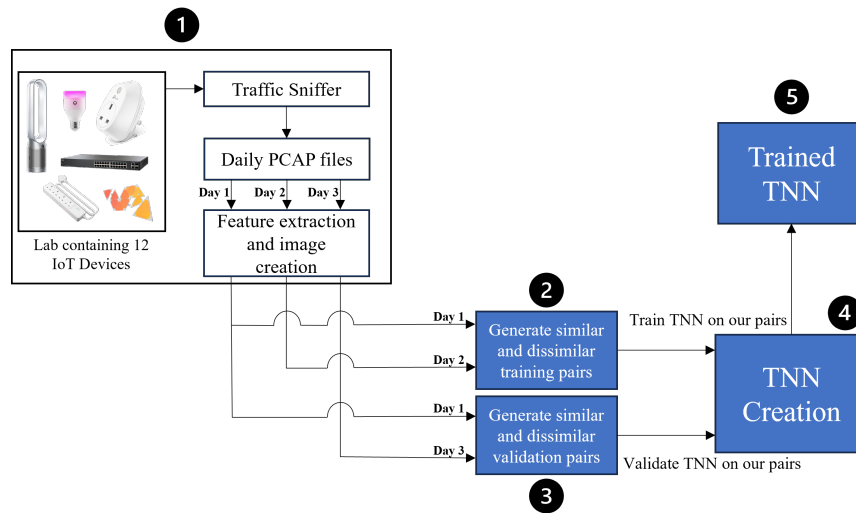


Fig. 7. System architecture for creating our TNN.

difference between the aggregated similarity scores for device pairs fed into the neural network between the reference and subsequent days. We consider 4 different indicators of accuracy:

- (1) All Samples: The percentage across all days considering all samples where they correctly show as 'similar'.
- (2) Majority Samples: The percentage of the days where the number of samples correctly shown as 'similar' is more than 'dissimilar' for each day.
- (3) Majority Mean Threshold: The percentage of the days where the mean of all the samples is above the chosen threshold value of 0.5.
- (4) Hedges' g: The percentage of the days where the Hedges' g score of the mean of all the samples is above the chosen effect size value of 0.5 and positive.

We use Hedges' g due to the fact it doesn't require the datasets to be normally distributed, which in our case holds true as we would expect our reference day values to all be close to either 0 or 1 if the TNN is working correctly. Because of not always having 900 samples, we then need to use Hedges' g as it accounts for biases introduced with small sample sizes and is therefore useful when comparing our datasets that may have a different number of samples (Hedges' g is generally useful when the number of samples is less than 50). When using our TNN, the expectation is that the device input images are dissimilar enough to be classified using the default similarity threshold of 0.5 for similar or dissimilar. This may hold true for different device models, but with device versions it is likely that the change will be more subtle and therefore unlikely that this would result in a large similarity score change, above the 0.5 threshold. This allows us to understand whether our technique is stable for experiment 1 and can detect changes for experiment 2, and how different measures of accuracy perform. As we vary the dissimilar images randomly, we will perform 10 runs, giving rise to 10 different created TNNs, to see how stable the results are.

Our full end-to-end system for testing our TNN is shown in Fig. 8. Our IoT lab traffic is sniffed to generate PCAP files per device, which then allows feature extraction and image creation for 11 days (1). For every device, pairings for day 1 to days 4, 5 6 and 7 are generated as similar pairs (same version) and pairings for days 1 to days 8, 9, 10 and 11 are

generated as dissimilar pairs (version change) (2). These are both passed in the previously trained TNN (3) with the intention to show that the TNN can detect stable versions per device (4) and version changes (5).

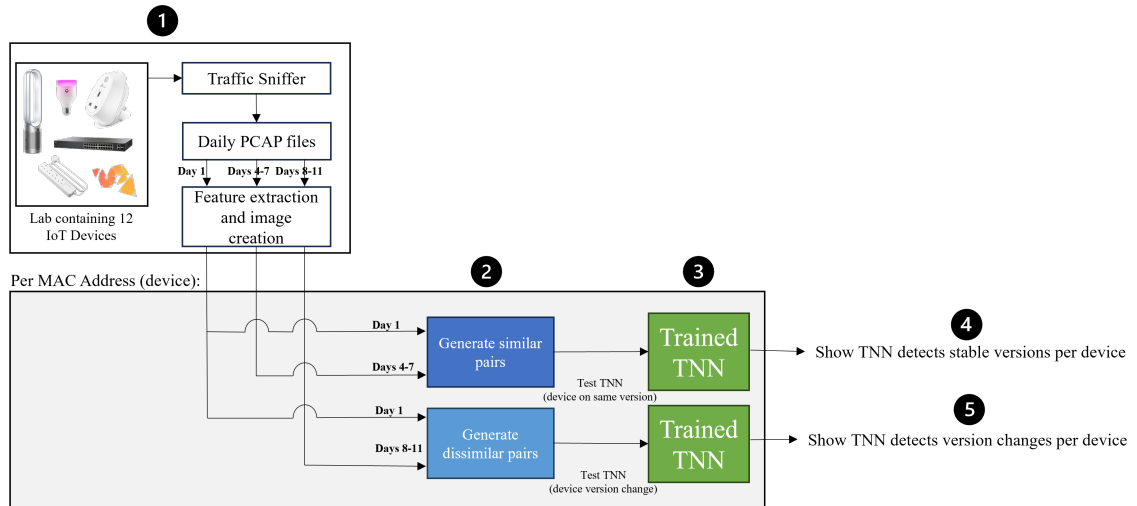


Fig. 8. System architecture for testing the trained TNN with two experiments.

## 5 RESULTS

We first review the results of our two experiments at a high level, with a more in-depth discussion of the results in the section 6. We will consider the results across our 10 runs generally.

### 5.1 Training and Validating the TNNs

When training our TNNs, we have 1800 possible pairs for training – 900 similar and 900 dissimilar – for our time window size across our time period. For our training set, we found that this maximum number holds true for all except one device. Our Hoze device only had 484 samples, meaning only just over half of the timeslots had data. For our validation set, we found again that our Hoze device had 484 samples, but also our Cisco SG200 device had slightly less than 900 with 840 samples. This however is still enough to train the TNNs adequately as we ended up with 20768 samples in total to train our TNNs, and 20648 samples for validation. For each of the 10 models we train, the similar pairs are always the same and we vary the dissimilar images (although there are always a maximum of 900 of each per device). The distribution of our training pairs for our highest performing run, and also the main mis-classifications are shown in Fig. 9.

The overall results of training our TNNs are shown in Table 3. We can see that through 10 separate iterations of TNN training with varied dissimilar images the accuracy and loss scores for all samples (both similar and dissimilar images) are all at around 99%. This shows our technique generally works and the TNNs can distinguish between similar and dissimilar pairs well. Note that these results are with the TNN using a default threshold of 0.5 for a similarity decision. For our specific use case, we are interested only in the similar pairs to see whether the technique works well enough to correctly identify similar images for devices. This is analogous to one device with one MAC address working as expected, with a stable version. Considering just the similar pairs again, the TNNs score highly at approximately 99%.

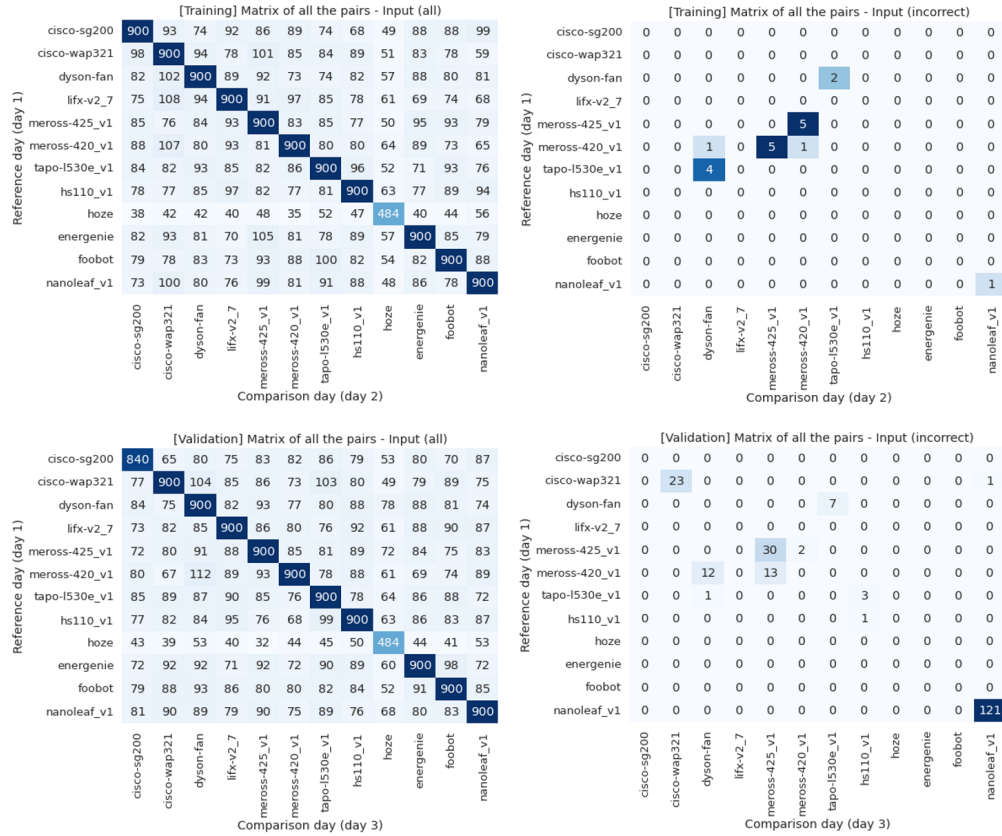


Fig. 9. Training (top left) and validation (bottom left) image distribution for run 4, including mis-classifications for training (top right) and validation (bottom right).

From these results we would expect our TNNs to perform well at identifying stable device versions when comparing subsequent days of unseen data to the day 1 baseline. We may also expect it to perform fairly well on completely unseen and different data (version change data), as it should pick up the nuances in version difference due to the small loss values. Based on the validation results in Fig. 9, we may expect the TNN to perform worst with the Nanoleaf Shapes device, with some other misclassifications occurring sporadically too.

	R1	R2	R3	R4	R5	R6	R7	R8	R9	R10	Average
Training Loss (All Samples)	0.0020	0.0025	0.0020	0.0015	0.0028	<b>0.0008</b>	0.0010	0.0010	0.0029	0.0026	0.0019
Validation Loss (All Samples)	0.0096	0.0101	0.0095	0.0093	0.0108	0.0103	0.0065	<b>0.0059</b>	0.0103	0.0091	0.0091
Training Accuracy (All Samples)	0.9979	0.9970	0.9979	0.9982	0.9966	<b>0.9989</b>	0.9987	0.9988	0.9964	0.9968	0.9977
Training Accuracy (Similar Only)	0.9970	0.9937	0.9979	0.9994	0.9966	0.9979	<b>1.0000</b>	0.9999	0.9988	0.9998	0.9981
Validation Accuracy (All Samples)	0.9885	0.9881	0.9898	0.9896	0.9878	0.9893	0.9932	<b>0.9937</b>	0.9880	0.9896	0.9898
Validation Accuracy (Similar Only)	0.9774	0.9800	0.9841	0.9809	0.9827	0.9801	0.9873	<b>0.9891</b>	0.9787	0.9830	0.9823

Table 3. TNN training and validation accuracy and loss for each of the 10 runs, to 4 decimal places. The run with the highest result per metric is shown in bold.

## 5.2 Stable Version Test

In the first experiment we test whether our trained TNN can successfully identify stable device versions. The input pairings are day 1 paired with days 4, 5, 6 and 7, which are unseen data but for known classes. Our overall accuracy results are shown in Table 4, and we now go through each of our accuracy metrics in turn. We see when considering all similar samples in our test data we get an accuracy similar to our training accuracy, showing we have not overfit our TNN on the training and validation data. With majority voting we see that using either the majority samples or majority mean threshold method gives a very accurate score. This is perhaps expected given the training results had high accuracy and very small loss, with a high number of samples per class. This means any incorrect values would essentially be ignored as outliers. Hedges’ g scores lowest for this experiment but still scores above 90% in most cases. This shows that generally the mean similarity score is consistent across days. With a larger effect size noted, the average mean would be quite different between training and testing as noticed by Hedges’ g, but not large enough to be above the 0.5 threshold.

	R1	R2	R3	R4	R5	R6	R7	R8	R9	R10	Average
Mean Threshold	<b>100%</b>	<b>100%</b>	<b>100%</b>	<b>97.92%</b>	<b>100%</b>	<b>100%</b>	<b>100%</b>	<b>100%</b>	<b>100%</b>	<b>100%</b>	<b>99.79%</b>
Majority Samples	<b>100%</b>	<b>100%</b>	<b>100%</b>	<b>97.92%</b>	<b>100%</b>	<b>100%</b>	<b>100%</b>	<b>100%</b>	<b>100%</b>	<b>100%</b>	<b>99.79%</b>
All Samples	97.97%	98.59%	99.07%	96.62%	98.79%	98.84%	98.63%	98.92%	98.23%	97.76%	98.34%
Hedges	89.58%	93.75%	95.83%	91.67%	87.50%	<b>95.83%</b>	91.67%	93.75%	89.58%	87.50%	91.67%

Table 4. TNN testing results across the 10 runs for our four different measures of accuracy when identifying stable versions.

	TNN Worst Identification (Nanoleaf Shapes)	TNN Best Identification (Energenie)
Baseline Samples	898/2	900/0
Validation Samples	777/123	900/0
Testing Samples	440/460 483/417 862/38 876/24	887/13 900/0 900/0 900/0
Baseline Mean	0.0089	0.0001
Validation Mean	0.1388	0.0002
Testing Means	0.5187 0.4552 0.0410 0.0318	0.0497 0.0001 0.0002 0.0001
Hedges Testing Scores	1.6676 1.4745 0.2790 0.2434	0.4875 0.1051 0.5325 -0.1263

Table 5. Statistics for the TNN performance across different devices.

We can further analyse our results in detail. Our TNN performed poorly at identifying the Nanoleaf Shapes device. If we concentrate on the results from run 4, where the TNN generally performed poorly across all accuracy measures in testing (shown in Table 5), we can note the following. In terms of the number of samples above and below the 0.5 similarity threshold, with our training, or baseline set, the model correctly identified almost all 900 samples (898), whereas in validation this number dropped to 777, and subsequently further dropped in testing where it identified



440 correctly and 460 incorrectly in the worst case. This however will only affect the ‘all samples’ accuracy, as due to majority voting with samples, our ‘majority samples’ accuracy would ignore those outliers. When considering the mean we see the baseline score was 0.0089, whereas in validation this rose to 0.1388, and over 0.5 in testing. This then affected the Hedges’ g result, scoring 1.6676, showing a very large effect. We can also look where our TNN performed well - identifying our Energenie device. We see in both training and unseen validation data that all 900 samples are correctly scored below the 0.5 threshold. Generally this holds true for testing too, the worst performance being 887 of 900 classified correct.

We also see that the baseline, validation and testing mean are generally similar, except for that first testing day, at around 0.0001. The Hedges’ g effect size is small in two cases and large in two others, which may be expected on our worst performing run. We can see that generally our technique works, although for same version identification, majority voting performs best.

### 5.3 Version Change Test

The second experiment was to use our TNN to identify when a device had changed version. Our TNN instances have only been trained on single versions per device, they have not been trained on different versions and so these are truly unknown images for the TNN to compute the similarity of. We use the same 4 accuracy measures here. Our first observation is that using a threshold of 0.5 as standard for a TNN does not work. If we use a standard threshold either with all samples, majority samples or majority mean threshold, our score is always less than the Hedges’ g score, and also less than 50% accurate. Generally the Hedges’ g value is approximately 20% more accurate than the other standard accuracy measures.

	R1	R2	R3	R4	R5	R6	R7	R8	R9	R10	Average
Mean Threshold	34.38%	25.00%	25.00%	46.88%	25.00%	34.38%	50.00%	37.50%	46.88%	28.13%	35.31%
Majority Samples	25.00%	25.00%	25.00%	40.63%	25.00%	34.38%	50.00%	37.50%	46.88%	28.13%	33.75%
All Samples	32.00%	27.16%	29.29%	44.12%	31.06%	35.63%	48.18%	31.20%	45.08%	37.59%	36.13%
Hedges’ g	<b>68.75%</b>	<b>65.63%</b>	<b>84.38%</b>	<b>75.00%</b>	<b>75.00%</b>	<b>62.50%</b>	<b>65.63%</b>	<b>62.50%</b>	<b>81.25%</b>	<b>71.88%</b>	<b>71.25%</b>

Table 6. TNN testing results across the 10 runs for our four different measures of accuracy when identifying version changes.

Further analysing the results, picking out some of the results from run 4 day 5 - our TNN performed worst at identifying the Tapo L530e device which had all samples marked as incorrect. We see that even when the version has changed, the mean for the baseline and testing is very similar, showing that any change the device has between versions is not noticeable on the wire for our technique (or possibly for any technique). Our Hedges’ g score also shows a small effect size, indicating the testing images are similar. Our next observation is the LIFX A19 which only had a subtle change to the TNN. We see here that using the samples accuracy metric, only 72 of the 900 are scored as above 0.5, and therefore classed as different, which is a poor score. This is further shown by the testing mean being 0.833, which, although higher than the baseline of 0.00003, is not high enough to be classed by a standard TNN as different enough. However, when we use Hedges’ g, we see the change in mean is classed as significant - an effect size of over 0.5. For this set of data, Hedges’ g is therefore the best measure to use. This is likely to be the reason for the 20% difference in accuracy scores in Table 6. Our final observation is for devices that have changed by a large amount. Our TNN scored highly on all accuracy metrics when identifying the TPLink HS110 device. The mean had gone from 0.0006 to 0.9960, showing a high difference in similarity. This aligns to both the samples, which all were classed as ‘dissimilar’

and the Hedges’ g score being over 66 (when our threshold for difference is only 0.5). We can conclude the following: Hedges’ g can be the most useful accuracy metric for version changes, as it can pick up both large differences and subtle differences, and is shown to be, on average, 20% more accurate than the standard TNN measure. Hedges’ g is therefore needed for version change identification as some device version changes are hugely different when others are subtle. This is therefore potentially a solution to the problem of identifying device version changes.

	Worst Performing (Tapo L530e)	Subtle change (LIFX A19)	Best performing (TP-Link HS110)
Baseline Samples	900/0	900/0	900/0
Testing Samples	900/0	828/72	0/900
Baseline Mean	0.0005	0.00003	0.0006
Testing Mean	0.0010	0.0833	0.9960
Hedges Score	0.0761	0.5349	66.7936

Table 7. Statistics for the worst, subtle change and best performing examples regarding version changes.

## 6 RESULTS ANALYSIS AND DISCUSSION

We will now discuss the results from the previous section in more detail and analyse possible reasons for the results, again discussing generally across the 10 runs.

### 6.1 Training and Validating the TNNs

When training our TNN, it was shown that our input data was relatively balanced - all but 1 device had the full 900 samples available for testing, and all but 2 had the full 900 samples available for validation. We also saw that training and validation yielded similar results of a high accuracy of over 99% in cases of all samples (dissimilar and similar) and similar only. When looking at the similar input images for training, we can see why our technique of using a TNN with image similarity works and produces a high accuracy score. Figure 10 shows one of the training pairs for the Energenie device. The figure shows the images are similar in the sense that only 3 protocols are shown to be in use - UDP, DNS and ICMP. The green circles show the subtle differences between the images - within the ‘time period’ features in the left hand side image have more variance between the values, noted by the change in greyscale, whereas the right hand side image values are all approximately the same as they are all white. These subtle differences are what the TNN uses to identify devices, and why our mean similarity score was not exactly 0 (and is very unlikely to be).

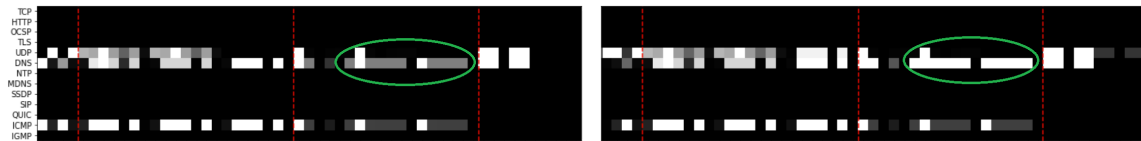


Fig. 10. Visualisation of Energenie similar training pairs.

In terms of dissimilar images, we needed to ensure that the images were clearly dissimilar between devices. In Fig. 11 the Tapo L530e and Nanoleaf Shapes devices do produce quite dissimilar images with features that the TNN would identify. Both devices used TCP and TLS protocols which had varying packet rates and magnitudes, however the Tapo L530e device (LHS of Fig. 11) had ICMP packets whereas the Nanoleaf Shapes device (RHS of Fig. 11) uses NTP and

mDNS more frequently. If we compare these two images to the ones for the Energenie device in Fig. 10 we can see the images are all distinct per device.

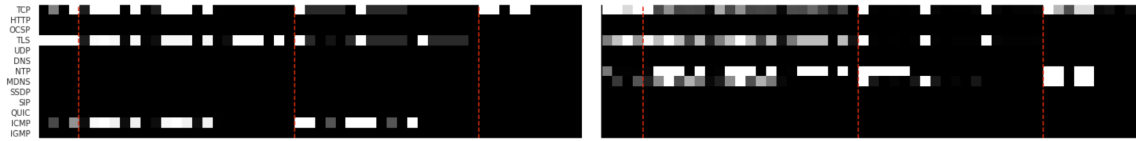


Fig. 11. visualisation of Tapo L530e vs Nanoleaf Shapes dissimilar training pairs.

We did notice a small number of mis-classifications across training and validation, both false positive, where dissimilar samples were classed as similar, and false negative, where similar samples were classed as dissimilar. Starting with the false positive shown in Fig. 13, we see for this sample that the Dyson Fan device (LHS of Fig. 12) and the Tapo L530e device (RHS of Fig. 12) do indeed look very similar, with our technique outputting a score of 0.021 for these images, which aligns to the fact that some pixels have a slightly different colour. We can see however that these cases didn't affect the technique much, due to this only being a very small number of samples in both training and validation. For the false negative, we have samples from the Nanoleaf Shapes device, which the TNN does not perform well at identifying in either training or validation. We can see in Fig. 13 how this device does not have an overly consistent fingerprint. For the TCP, TLS and mDNS protocols they look vaguely similar across samples. However the first sample also uses more uDP, SSDP and ICMP, making it look quite different, noted by the score given of 0.579, just over the threshold of being similar.



Fig. 12. An example false positive - the two different device images (Dyson Fan and Tapo L530e) were erroneously classed by the TNN as similar.



Fig. 13. An example false negative - the two different device images from the same device (Nanoleaf Shapes) were erroneously classed by the TNN as dissimilar.

We have shown that our TNN produces a high accuracy score during training and validation and from analysis of the input images we can see why this is the case. Across our two days for training the images seem to be similar enough between sample periods for a device and dissimilar enough between different devices to distinguish them. We also explored the main misclassifications but note that they didn't affect the overall TNN accuracy by much. One thing worth exploring further here is around tweaking the TNN for potentially better results, for example if day 3 fails to get a high enough validation accuracy. We will expand on this further in Section 6.4.

## 6.2 Stable Version Test

We had four days worth of data to test our TNN at identifying devices with a stable version. In the results section we saw that our technique performed well for the Energenie device. If we look at the input images in Fig. 14 we can see why this is the case. The images shown are almost identical in terms of protocols used and magnitudes, so it makes sense that the TNN worked well in this case. We did however, again as expected, see that the TNN struggled with identification of the Nanoleaf Shapes device. If we look at those input images, specifically one that was misclassified in Fig. 15 we can see that the issue is not the trained TNN as it works as expected in terms of identifying that the images are different, the issue is that those images coming from the same device are quite different. We highlight some of the main differences between these two images, namely more protocols being used and magnitude of pixels being vastly different. We have shown however that our technique does work for device stable version identification, with any of the accuracy scores for the samples being useful as a metric.

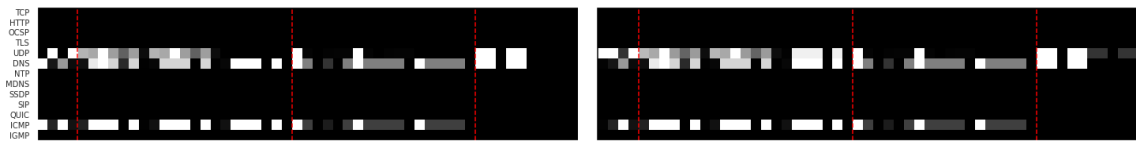


Fig. 14. Visualisation of Energenie device similar training pairs.

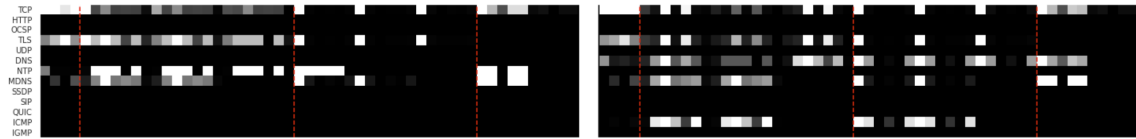


Fig. 15. Visualisation of Nanoleaf Shapes device similar training pairs.

## 6.3 Version Change Test

We now discuss the version change results, exploring further the results shown in Section 5.3. As mentioned, these images were unknown to the TNN during the training phase. Starting with a device that showed a large, obvious change (TPLink HS110), we see in Fig. 16 that the pattern is similar for TCP, TLS and ICMP traffic, however after the update more UDP traffic was seen. If we then compare the PCAPs of pre and post update (Fig. 17) we can see the main changes align. There is still TCP and TLS traffic however the number of bytes post update for these protocols has decreased. We also note that a new ‘TPLINK’ protocol is in use, which is based on UDP.

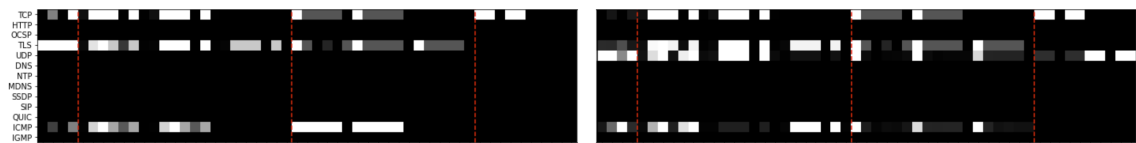


Fig. 16. TPLink HS110 input images for v1.0.10 (LHS) and v1.2.6 (RHS).

03:59:38...	192.168.4.55	192.168.4.150	ICMP	183	04:02:22...	192.168.49.106	192.168.49.114	TPLINK...	646
04:02:23...	192.168.4.55	ec2-52-30-70-189.eu-wes...	TLSv1	172	04:02:30...	192.168.49.106	ec2-52-209-205-164.eu-w...	TLSv1.2	130
04:02:23...	ec2-52-30-70-189.eu-wes...	192.168.4.55	TLSv1	135	04:02:30...	ec2-52-209-205-164.eu-w...	192.168.49.106	TLSv1.2	124
04:02:23...	192.168.4.55	ec2-52-30-70-189.eu-wes...	TCP	66	04:02:30...	192.168.49.106	ec2-52-209-205-164.eu-w...	TCP	66
04:06:19...	192.168.4.55	ec2-52-30-70-189.eu-wes...	TLSv1	172	04:02:40...	192.168.49.106	192.168.49.139	TPLINK...	646
04:06:19...	ec2-52-30-70-189.eu-wes...	192.168.4.55	TCP	66	04:02:40...	192.168.49.106	192.168.49.38	TPLINK...	646
04:06:19...	ec2-52-30-70-189.eu-wes...	192.168.4.55	TLSv1	135	04:02:40...	192.168.49.38	192.168.49.106	ICMP	590
04:06:19...	ec2-52-30-70-189.eu-wes...	192.168.4.55	TCP	135	04:03:22...	192.168.49.106	192.168.49.114	TPLINK...	646
04:06:19...	192.168.4.55	ec2-52-30-70-189.eu-wes...	TCP	78	04:03:39...	192.168.49.106	192.168.49.139	TPLINK...	646
04:10:15...	192.168.4.55	ec2-52-30-70-189.eu-wes...	TLSv1	172	04:03:39...	192.168.49.139	192.168.49.106	UDP	44
04:10:15...	ec2-52-30-70-189.eu-wes...	192.168.4.55	TCP	66	04:03:39...	192.168.49.106	192.168.49.139	ICMP	72
04:10:15...	ec2-52-30-70-189.eu-wes...	192.168.4.55	TLSv1	135	04:03:41...	192.168.49.106	192.168.49.38	TPLINK...	646
04:10:15...	192.168.4.55	ec2-52-30-70-189.eu-wes...	TCP	66	04:03:41...	192.168.49.38	192.168.49.106	ICMP	590

Fig. 17. Wireshark capture of the TPLink HS110 device v1.0.10 (LHS) and v1.2.6 (RHS).

We now look at the case where there were subtle differences picked up between device firmware versions, where Hedges’ g was needed over standard thresholds to notice this change. For this we saw the LIFX A19 device had subtle differences available between versions, picked up by the TNNs shown in Fig. 18. Fig. 19 shows the capture before and after the update. If we analyse the Wireshark captures between versions at approximately midnight when our first sample would be taken, we see that the LIFX device does broadly the same things for 12 packets - it has UDP, mDNS, TLS and TCP packets of the same size, plus a device on the local network pings the LIFX device. However we notice that post-update the LIFX device no longer pings the gateway (highlighted green in the figure) and just gets periodic pings to it. Our choice of devices meant that devices on the network would ping each other, but this is ok for two reasons. Even without them the LIFX version change would still be noticed as the LIFX stopped pinging the gateway, plus in a deployment the learned behaviours of the network would contribute to the baseline normal. This change aligns to the TNN greyscale image - prior to the update it was more balanced with grey pixels for server and client, after the update it became white and related to the server only.

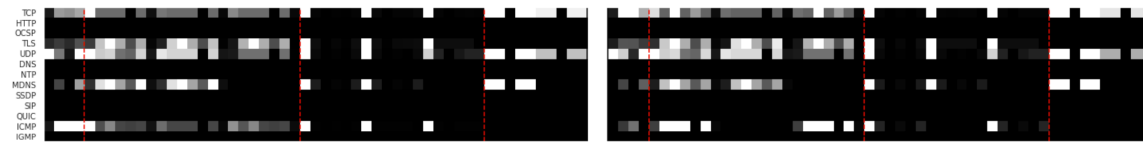


Fig. 18. LIFX A19 input image comparison between v2.7 (LHS) and v2.8 (RHS).

00:01:27...	Lifx-1.local	192.168.49.38	UDP	83	23:59:51...	Lifx-1.local	192.168.49.38	UDP	83
00:01:27...	192.168.49.38	Lifx-1.local	ICMP	111	23:59:51...	192.168.49.38	Lifx-1.local	ICMP	111
00:01:27...	Lifx-1.local	192.168.49.38	UDP	83	23:59:51...	Lifx-1.local	192.168.49.38	UDP	83
00:01:27...	192.168.49.38	Lifx-1.local	ICMP	111	23:59:51...	192.168.49.38	Lifx-1.local	ICMP	111
00:01:28...	Lifx-1.local	192.168.49.254	ICMP	58	23:59:56...	lb.lifx.co	Lifx-1.local	TLSv1.2	139
00:01:28...	192.168.49.254	Lifx-1.local	ICMP	58	23:59:56...	Lifx-1.local	lb.lifx.co	TCP	54
00:01:33...	Lifx-1.local	mdns.mcast.net	MDNS	188	23:59:56...	Lifx-1.local	lb.lifx.co	TLSv1.2	187
00:01:33...	Lifx-1.local	mdns.mcast.net	MDNS	188	23:59:56...	lb.lifx.co	Lifx-1.local	TCP	54
00:01:33...	Lifx-1.local	ff02::fb	MDNS	208	00:00:10...	Lifx-1.local	mdns.mcast.net	MDNS	188
00:01:33...	Lifx-1.local	ff02::fb	MDNS	208	00:00:10...	Lifx-1.local	mdns.mcast.net	MDNS	188
00:01:38...	Lifx-1.local	192.168.49.254	ICMP	58	00:00:10...	Lifx-1.local	ff02::fb	MDNS	208
00:01:38...	192.168.49.254	Lifx-1.local	ICMP	58	00:00:10...	Lifx-1.local	ff02::fb	MDNS	208
00:01:40...	Lifx-1.local	lb.lifx.co	TLSv1.2	139	00:00:11...	lb.lifx.co	Lifx-1.local	TCP	54
00:01:40...	lb.lifx.co	Lifx-1.local	TLSv1.2	139	00:00:11...	Lifx-1.local	lb.lifx.co	TCP	54
00:01:40...	Lifx-1.local	lb.lifx.co	TCP	54	00:00:12...	Lifx-1.local	192.168.49.139	UDP	83
00:01:40...	lb.lifx.co	Lifx-1.local	TCP	54	00:00:12...	Lifx-1.local	192.168.49.139	UDP	83

Fig. 19. Comparison of LIFX A19 v2.7 (LHS) and v2.8 (RHS) firmware version traffic captures.

For all 10 trained TNNs, The Tapo L530e version change did not get identified. Starting with the input images, taking Fig. 20 as an example, we see that they are essentially identical; there is no obvious difference between the two versions, which aligns to the average mean and Hedges’ g score in Section 5.3. If we then look at part of the Wireshark captures

that relate to these images (Fig. 21), we can see why this is the case. In both cases there is an exchange of 21 packets across TCP and TLS, followed by a (local) ICMP packet. These packets are all shown to be the same size, of 123, 127 and 60 bytes for the TCP and TLS exchange and 70 bytes for the ICMP request. The only differences between the versions is the source port number which appears random as expected, and the DNS hostname, but this is not a feature considered with flow techniques, and so no technique using flow statistics would work here. A keywords approach [4, 5] however might pick up this change if it was significant.

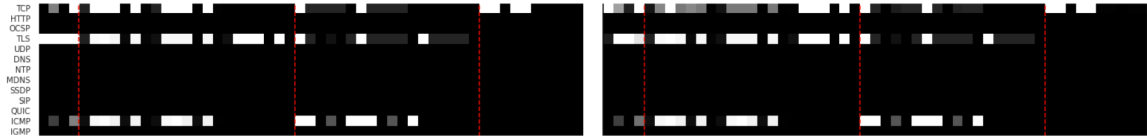


Fig. 20. Tapo L530e device showing no difference in input images across versions 1.2.2 (LHS) and 1.2.4 (RHS).

No.	Time	Source	Destination	Protocol	Length	No.	Time	Source	Destination	Protocol	Length
5	2023-08-02 00:01:03	172.16.32.200	prd-iot-cloudgateway-de-	TLSv1.2	123	53	2023-08-04 00:08:23	172.16.32.200	ec2-34-249-165-121.eu-w-	TLSv1.2	123
7	2023-08-02 00:01:04	prd-iot-cloudgateway-dev-	172.16.32.200	TLSv1.2	127	55	2023-08-04 00:08:23	ec2-34-249-165-121.eu-west-1.compute.amazona-	172.16.32.200	TLSv1.2	127
8	2023-08-02 00:01:04	172.16.32.200	prd-iot-cloudgateway-de-	TCP	60	56	2023-08-04 00:08:23	172.16.32.200	ec2-34-249-165-121.eu-w-	TCP	60
13	2023-08-02 00:03:02	172.16.32.200	prd-iot-cloudgateway-de-	TLSv1.2	123	61	2023-08-04 00:10:21	172.16.32.200	ec2-34-249-165-121.eu-w-	TLSv1.2	123
15	2023-08-02 00:03:02	prd-iot-cloudgateway-dev-	172.16.32.200	TLSv1.2	127	63	2023-08-04 00:10:21	ec2-34-249-165-121.eu-west-1.compute.amazona-	172.16.32.200	TLSv1.2	127
16	2023-08-02 00:03:02	172.16.32.200	prd-iot-cloudgateway-de-	TCP	60	64	2023-08-04 00:10:22	172.16.32.200	ec2-34-249-165-121.eu-w-	TCP	60
21	2023-08-02 00:05:00	172.16.32.200	prd-iot-cloudgateway-de-	TLSv1.2	123	69	2023-08-04 00:12:20	172.16.32.200	ec2-34-249-165-121.eu-w-	TLSv1.2	123
23	2023-08-02 00:05:00	prd-iot-cloudgateway-dev-	172.16.32.200	TLSv1.2	127	71	2023-08-04 00:12:20	ec2-34-249-165-121.eu-west-1.compute.amazona-	172.16.32.200	TLSv1.2	127
24	2023-08-02 00:05:01	172.16.32.200	prd-iot-cloudgateway-de-	TCP	60	72	2023-08-04 00:12:20	172.16.32.200	ec2-34-249-165-121.eu-w-	TCP	60
33	2023-08-02 00:06:59	172.16.32.200	prd-iot-cloudgateway-de-	TLSv1.2	123	81	2023-08-04 00:14:18	172.16.32.200	ec2-34-249-165-121.eu-w-	TLSv1.2	123
35	2023-08-02 00:06:59	prd-iot-cloudgateway-dev-	172.16.32.200	TLSv1.2	127	83	2023-08-04 00:14:18	ec2-34-249-165-121.eu-west-1.compute.amazona-	172.16.32.200	TLSv1.2	127
36	2023-08-02 00:06:59	172.16.32.200	prd-iot-cloudgateway-de-	TCP	60	84	2023-08-04 00:14:19	172.16.32.200	ec2-34-249-165-121.eu-w-	TCP	60
41	2023-08-02 00:08:57	172.16.32.200	prd-iot-cloudgateway-de-	TLSv1.2	123	89	2023-08-04 00:16:17	172.16.32.200	ec2-34-249-165-121.eu-w-	TLSv1.2	123
43	2023-08-02 00:08:57	prd-iot-cloudgateway-dev-	172.16.32.200	TLSv1.2	127	91	2023-08-04 00:16:17	ec2-34-249-165-121.eu-west-1.compute.amazona-	172.16.32.200	TLSv1.2	127
44	2023-08-02 00:08:57	172.16.32.200	prd-iot-cloudgateway-de-	TCP	60	92	2023-08-04 00:16:17	172.16.32.200	ec2-34-249-165-121.eu-w-	TCP	60
53	2023-08-02 00:10:56	172.16.32.200	prd-iot-cloudgateway-de-	TLSv1.2	123	101	2023-08-04 00:18:15	172.16.32.200	ec2-34-249-165-121.eu-w-	TLSv1.2	123
55	2023-08-02 00:10:56	prd-iot-cloudgateway-dev-	172.16.32.200	TLSv1.2	127	103	2023-08-04 00:18:15	ec2-34-249-165-121.eu-west-1.compute.amazona-	172.16.32.200	TLSv1.2	127
56	2023-08-02 00:10:56	172.16.32.200	prd-iot-cloudgateway-de-	TCP	60	104	2023-08-04 00:18:15	172.16.32.200	ec2-34-249-165-121.eu-w-	TCP	60
61	2023-08-02 00:12:54	172.16.32.200	prd-iot-cloudgateway-de-	TLSv1.2	123	109	2023-08-04 00:20:13	172.16.32.200	ec2-34-249-165-121.eu-w-	TLSv1.2	123
63	2023-08-02 00:12:54	prd-iot-cloudgateway-dev-	172.16.32.200	TLSv1.2	127	111	2023-08-04 00:20:14	ec2-34-249-165-121.eu-west-1.compute.amazona-	172.16.32.200	TLSv1.2	127
64	2023-08-02 00:12:55	172.16.32.200	prd-iot-cloudgateway-de-	TCP	60	112	2023-08-04 00:20:14	172.16.32.200	ec2-34-249-165-121.eu-w-	TCP	60
75	2023-08-02 00:13:21	172.16.32.200	172.16.34.135	ICMP	70	125	2023-08-04 00:22:02	172.16.32.200	172.16.34.135	ICMP	70

Fig. 21. Tapo L530e device showing no on-wire differences between version 1.2.2 (LHS) and 1.2.4 (RHS).

It is worth stating that on-wire changes may not be directly related to change in the firmware between versions. During a device update a device may reboot and refresh any internal configuration, or re-advertise itself on the network, making devices interact again. This is still useful however, as identifying this can also lead towards anomaly detection techniques for traffic between devices.

#### 6.4 Proposed Real World Architecture

We have shown that we have a viable technique that can identify when a device is on a stable version, and also when it changes version. This technique can also be expanded to identify device models and perform anomaly detection. It is worth discussing how our technique could be enhanced to be deployed for real-world use. Our technique could be deployed as a system in the following way as shown in Fig. 22. We propose a cloud-based approach where a solution in the cloud would have access to all device fingerprints, and a constantly updating database of latest versions of devices. This could either be from relationships with manufacturers, monitoring websites or obtaining devices and manually checking versions. This then allows a large database of fingerprint images of what the devices should look like under normal use, running a specific firmware version, as a baseline to compare images from other networks against. This cloud-based approach would then allow fingerprints per device to be pushed down to users, to train their own ML model specific to their network. This allows the model to use both the known good fingerprints from the cloud plus

any nuances to their home network, for example how devices on the LAN interact with each other. This trained model could then form the basis of an app, with results specific to each user. The tool would work in the following way:

- If no change in device behaviour is detected, the device is presumed to be up to date.
- If change is detected, the cloud service is queried.
- If the response of this query says that there is a new latest version available for the device, it is presumed that the device must have updated. The model is therefore re-trained with new traffic. This can optionally be flagged to the user to confirm.
- If there is no new version available, the device behaviour is considered anomalous, so manual checking of the device and its traffic is required. This would be flagged to the user.
- If this manual checking finds a genuine compromise, the device is disabled and fixed/permanently removed; otherwise the model is re-trained.

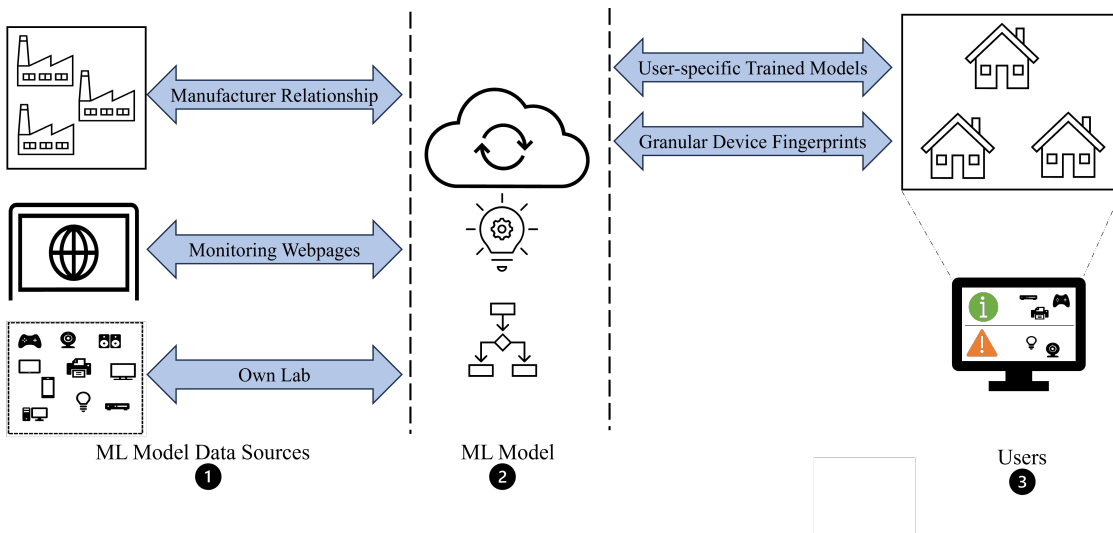


Fig. 22. Graphical depiction of a real-world tool for automated version identification.

This cloud based approach is similar to the products (Fingbox, Bitdefender BOX2) mentioned in [6], but our technique could enhance their capabilities. To align with other products available, such as Amazon IoT Device Defender [2], or Microsoft Defender for IoT [26] we would want to implement model re-training. Our current method uses days 1 and 2 data for training and day 3 for validation. If it was found that day 3 did not validate the model well (anomalies were detected erroneously) we could consider using more data to improve the model. For example we could use day 4 for validation against training on days 1 and 2, or re-training on days 2 and 3 with validation on day 4. We could also implement something like a ‘7 day rolling score’ with a report to users on which days had been flagged as anomalous. It may be the case that single days were anomalous and then normal again, and it would be up to the user to look into this further if they wish. This still provides an efficiency gain for users, notifying them of a small number of devices that need checking.

## 7 CONCLUSIONS AND FUTURE WORK

In this paper we identified two challenges for identifying IoT firmware versions: the on-wire behaviour resulting from different firmware versions running on the same device are more subtle than those for different device models, types or manufacturers; and there is limited data on different device versions due to lack of publicly available datasets. These challenges are novel in this area and have therefore not previously been addressed by the literature. We developed a technique using flow statistics to transform on-wire device behaviours into greyscale images. These images were fed into a Twin Neural Network model to output similarity scores. Our best performing model was 95.83% accurate at identifying stable versions and 84.38% accurate identifying version changes. By calculating the Hedges'  $g$  effect size of similarity scores, we were able to detect the subtle changes resulting from a device running different firmware versions. We showed how Hedge's  $g$  as a metric is approximately 20% more accurate than the standard TNN measure. By using a TNN model trained on device differences – but tested on version changes – we were able to overcome the limited data problem via transfer learning. This allowed the TNN to be able to correctly calculate the similarity of images that were truly unknown - the images of different device versions had not been used to train the TNN.

To improve our technique, further work could be carried out in this area, including:

- (1) Using active approaches. Although stated to not be ideal for the reasons mentioned in the introduction, active approaches may have a place in augmenting techniques when identifying device versions to overcome the problem when a device has no change in passive on-wire signature. This could either be from banner grabbing on known ports (as the version change may update versions or banners of extra components such as libraries), or logging into device management pages and identifying version strings.
- (2) Using this technique to identify newly added devices, or expanding to a huge database of known devices as an identification technique for unknown devices.
- (3) We have shown our technique can identify anomalies in terms of version changes, there would be value in applying the same technique for other types of anomaly detection from compromised devices.

## REFERENCES

- [1] Georgios Agrafiotis, Eftychia Makri, Ioannis Flionis, Antonios Lalas, Konstantinos Votis, and Dimitrios Tzovaras. 2022. Image-based Neural Network Models for Malware Traffic Classification using PCAP to Picture Conversion. 17th International Conference on Availability, Reliability and Security.
- [2] Amazon Web Services. 2024. AWS IoT Device Defender FAQs. <https://aws.amazon.com/iot-device-defender/faq/> [Accessed: 07.04.2024].
- [3] Nesrine Ammar, Ludovic Noirie, and Sebastien Tixeul. 2020. Autonomous Identification of IoT Device Types based on a Supervised Classification. International Conference on Communications (ICC).
- [4] Ashley Andrews, George Oikonomou, Simon Armour, Paul Thomas, and Thomas Cattermole. 2023. Granular IoT Device Identification Using TF-IDF and Cosine Similarity. Proceedings of the 5th Workshop on CPS&IoT Security and Privacy. , 9 pages.
- [5] Ashley Andrews, George Oikonomou, Simon Armour, Paul Thomas, and Thomas Cattermole. 2023. Keyword Extraction for Fine-Grained IoT Device Identification. 2022 Seventh International Conference on Fog and Mobile Edge Computing (FMEC).
- [6] Ashley Andrews, George Oikonomou, Simon Armour, Paul Thomas, and Thomas Cattermole. 2023. Reliable Identification of IoT Devices from Passive Network Traffic Analysis: Requirements and Recommendations. World Forum on Internet of Things.
- [7] BBC. 2017. *How hackers could use doll to open your front door*. <https://www.bbc.co.uk/news/av/technology-38966285>. [Accessed: 07.04.2024].
- [8] BBC. 2020. *Smart doorbells 'easy target for hackers' study finds*. <https://www.bbc.co.uk/news/technology-55044568>. [Accessed: 07.04.2024].
- [9] BBC. 2023. *The tech flaw that lets hackers control surveillance cameras*. <https://www.bbc.co.uk/news/technology-65975446> [Accessed: 07.04.2024].
- [10] Punam Bedi, Neha Gupta, and Vinita Jindal. 2020. Siam-IDS: Handling class imbalance problem in Intrusion Detection Systems using Siamese Neural Network. *Procedia Computer Science*. , 780-789 pages.
- [11] Jane Bromley, Isabelle Guyon, Yann LeCun, Eduard Säckinger, and Roopak Shah. 1993. Signature Verification using a "Siamese" Time Delay Neural Network. *Advances in Neural Information Processing Systems*.
- [12] Luigi Catuogno and Clemente Galdi. 2023. Secure Firmware Update: Challenges and Solutions. *Cryptography* 7, 2 (2023), 1–17.
- [13] Batyr Charyyev and Mehmet Hadi Gunes. 2021. Locality-Sensitive IoT Network Traffic Fingerprinting for Device Identification. *IEEE Internet of Things Journal* 8 (2021), 1272–1281. Issue 3.



- [14] Cyfirma. 2022. Thousands of Hikvision Cameras are still vulnerable and can be potentially exploited. <https://www.cyfirma.com/research/thousands-of-hikvision-cameras-are-still-vulnerable-and-can-be-potentially-exploited> [Accessed: 07.04.2024].
- [15] Sounak Dey, Anjan Dutta, J. Ignacio Toledo, Suman K. Ghosh, Josep Lladós, and Umapada Pal. 2017. SigNet: Convolutional Siamese Network for Writer Independent Offline Signature Verification. arXiv. arXiv:1707.02131
- [16] Sergey Golubev, Evgenia Novikova, and Elena Fedorchenko. 2022. Image-Based Approach to Intrusion Detection in Cyber-Physical Objects. Information (Switzerland).
- [17] Hanan Hindy, Christos Tachtatzis, Robert Atkinson, Ethan Bayne, and Xavier Bellekens. 2021. Developing a Siamese Network for Intrusion Detection Systems. Proceedings of the 1st Workshop on Machine Learning and Systems, EuroMLSys 2021. , 120-126 pages. Issue 1.
- [18] Faisal Hussain, Syed Ghazanfar Abbas, Ivan Miguel Pires, Sabeeha Tanveer, Ubaid U. Fayyaz, Nuno M. Garcia, Ghalib A. Shah, and Farrukh Shahzad. 2021. A Two-Fold Machine Learning Approach to Prevent and Detect IoT Botnet Attacks. *IEEE Access* 9 (2021), 163412–163430.
- [19] Solaiman Kabir, Sadman Sakib, Md Akib Hossain, Safi Islam, and Muhammad Iqbal Hossain. 2021. A Convolutional Neural Network based Model with Improved Activation Function and Optimizer for Effective Intrusion Detection and Classification. *2021 International Conference on Advance Computing and Innovative Technologies in Engineering, ICACITE 2021* 7 (2021), 373–378.
- [20] Gregory Koch, Richard Zemel, and Ruslan Salakhutdinov. 2015. Siamese Neural Networks for One-shot Image Recognition.
- [21] Jaidip Kotak and Yuval Elovici. 2020. IoT device identification using deep learning. arXiv.
- [22] Hyun Kyo Lim, Ju Bong Kim, Kwihoon Kim, Yong Geun Hong, and Youn Hee Han. 2019. Payload-based traffic classification using multi-layer LSTM in software defined networks. Applied Sciences (Switzerland).
- [23] Samuel Marchal, Markus Miettinen, Thien Duc Nguyen, Ahmad Reza Sadeghi, and N. Asokan. 2019. AuDI: Toward Autonomous IoT Device-Type Identification Using Periodic Communication. *IEEE Journal on Selected Areas in Communications* 37 (2019), 1402–1412. Issue 6.
- [24] Yair Meidan, Michael Bohadana, Asaf Shabtai, Martin Ochoa, Nils Ole Tippenhauer, Juan Davis Guarnizo, and Yuval Elovici. 2017. Detection of Unauthorized IoT Devices Using Machine Learning Techniques. arxiv.
- [25] Yair Meidan, Vinay Sachidananda, Hongyi Peng, Racheli Sagron, Yuval Elovici, and Asaf Shabtai. 2020. A novel approach for detecting vulnerable IoT devices connected behind a home NAT. *Computers and Security* , 101968 pages.
- [26] Microsoft. 2024. Microsoft Defender for IoT. <https://www.microsoft.com/en-gb/security/business/endpoint-security/microsoft-defender-iot> [Accessed: 07.04.2024].
- [27] Nizar Msadek, Ridha Soua, and Thomas Engel. 2019. IoT Device Fingerprinting: Machine Learning based Encrypted Traffic Analysis. IEEE Wireless Communications and Networking Conference, WCNC.
- [28] Madushi H. Pathmaperuma, Yogachandran Rahulamathavan, Safak Dogan, and Ahmet Kondo. 2022. CNN for User Activity Detection Using Encrypted In-App Mobile Data. Future Internet.
- [29] Roberto Perdisci, Thomas Papastergiou, Omar Alrawi, and Manos Antonakakis. 2020. IoTFinder: Efficient Large-Scale Identification of IoT Devices via Passive DNS Traffic Analysis. Proceedings - 5th IEEE European Symposium on Security and Privacy, Euro S and P 2020. , 474-489 pages.
- [30] Shlomo S. Sawilowsky. 2009. Very large and huge effect sizes. *Journal of Modern Applied Statistical Methods* 8, 2 (2009), 597–599.
- [31] Arunan Sivanathan. 2020. *IoT behavioral monitoring via network traffic analysis*. Ph. D. Dissertation. UNSW.
- [32] Arunan Sivanathan, Hassan Habibi Gharakheili, Franco Loi, Adam Radford, Chamith Wijenayake, Arun Vishwanath, and Vijay Sivaraman. 2019. Classifying IoT Devices in Smart Environments Using Network Traffic Characteristics. *IEEE Transactions on Mobile Computing* 18, 8 (2019), 1745–1759.
- [33] Shayan Taheri, Milad Salem, and Jiann Shiun Yuan. 2018. Leveraging image representation of network traffic data and transfer learning in botnet detection. *Big Data and Cognitive Computing* 2, 4 (2018), 1–16.
- [34] Oliver Thompson, Anna Maria Mandalari, and Hamed Haddadi. 2021. Rapid IoT device identification at the edge. DistributedML 2021 - Proceedings of the 2nd ACM International Workshop on Distributed Machine Learning, Part of CoNEXT 2021. , 22–28 pages.
- [35] Fouad Trad, Ali Hussein, and Ali Chehab. 2023. Using Siamese Neural Networks for Efficient and Accurate IoT Device Identification. 2022 Seventh International Conference on Fog and Mobile Edge Computing (FMEC).
- [36] UK Parliament. 2023. Connected tech: smart or sinister? <https://publications.parliament.uk/pa/cm5803/cmselect/cmcomeds/157/report.html> [Accessed: 07.04.2024].
- [37] Yong Wang, Bhaskar P. Rimal, Mark Elder, Sofia I. Crespo Maldonado, Helen Chen, Carson Koball, and Kaushik Ragothaman. 2022. IoT Device Identification Using Supervised Machine Learning. Digest of Technical Papers - IEEE International Conference on Consumer Electronics.
- [38] David B Wilson. 2017. Formulas Used by the “ Practical Meta-Analysis Effect Size Calculator ”. George mason university.
- [39] Jingliang Xue, Yingchun Chen, Ou Li, and Fei Li. 2020. Classification and identification of unknown network protocols based on CNN and T-SNE. Classification and identification of unknown network protocols based on CNN and T-SNE. *Journal of Physics: Conference Series*.
- [40] Yifeng Zheng, Arindam Pal, Sharif Abuadbbba, Shiva Raj Pokhrel, Surya Nepal, and Helge Janicke. 2020. Towards IoT Security Automation and Orchestration. 2020 IEEE International Conference on Trust, Privacy and Security in Intelligent Systems and Applications (TPS-ISA).

## A EXTENDED STABLE VERSION RESULTS

Table 8. Number of samples that are below (left of bracket) and above (right of bracket) the 0.5 threshold for each of the 10 runs over each of the four days per device.

Device	Day	R1	R2	R3	R4	R5	R6	R7	R8	R9	R10
Cisco SG200	4	900/0	900/0	900/0	900/0	900/0	900/0	900/0	900/0	900/0	900/0
	5	900/0	900/0	900/0	900/0	900/0	900/0	900/0	900/0	900/0	900/0
	6	840/0	840/0	840/0	840/0	840/0	840/0	840/0	840/0	840/0	840/0
	7	900/0	900/0	900/0	900/0	900/0	900/0	900/0	900/0	900/0	900/0
Cisco WAP321	4	900/0	900/0	900/0	900/0	900/0	900/0	900/0	900/0	900/0	900/0
	5	900/0	900/0	900/0	900/0	900/0	900/0	900/0	900/0	900/0	900/0
	6	859/41	867/33	882/18	868/32	890/10	848/52	898/2	900/0	885/15	877/23
Dyson Fan	4	900/0	900/0	900/0	900/0	900/0	900/0	900/0	900/0	900/0	900/0
	5	900/0	900/0	900/0	900/0	900/0	900/0	900/0	900/0	900/0	900/0
	6	899/1	900/0	900/0	900/0	899/1	899/1	900/0	900/0	900/0	900/0
LIFX A19	4	900/0	900/0	900/0	900/0	900/0	900/0	900/0	900/0	900/0	900/0
	5	831/69	900/0	897/3	900/0	850/50	892/8	900/0	900/0	878/22	885/15
	6	843/57	900/0	841/59	900/0	894/6	893/7	900/0	900/0	841/59	895/5
MeRoss-425	4	870/30	900/0	870/30	900/0	870/30	870/30	900/0	870/30	870/30	870/30
	5	870/30	840/60	900/0	840/60	896/4	870/30	840/60	900/0	900/0	900/0
	6	837/63	784/116	840/60	752/148	840/60	840/60	780/120	812/88	840/60	840/60
MeRoss-420	4	892/8	879/21	898/2	899/1	887/13	898/2	900/0	900/0	890/10	900/0
	5	886/14	838/62	900/0	863/37	887/13	899/1	887/13	898/2	859/41	900/0
	6	890/10	862/38	897/3	887/13	878/22	899/1	900/0	897/3	856/44	889/11
Tapo L530e	4	900/0	900/0	900/0	900/0	900/0	900/0	900/0	900/0	900/0	900/0
	5	900/0	900/0	900/0	900/0	900/0	900/0	900/0	900/0	900/0	900/0
	6	842/28	869/1	870/0	852/18	870/0	870/0	846/24	847/23	869/1	843/27
TPLink HS110	4	899/1	900/0	900/0	900/0	899/1	900/0	900/0	900/0	900/0	900/0
	5	900/0	900/0	900/0	900/0	900/0	900/0	900/0	900/0	900/0	900/0
	6	900/0	899/1	900/0	900/0	900/0	900/0	900/0	900/0	898/2	900/0
Hoze	4	484/0	484/0	484/0	484/0	484/0	484/0	484/0	484/0	484/0	484/0
	5	484/0	484/0	484/0	484/0	484/0	484/0	484/0	484/0	484/0	484/0
	6	506/0	506/0	506/0	506/0	506/0	506/0	506/0	506/0	506/0	506/0
Energenie	4	838/62	900/0	900/0	887/13	888/12	888/12	900/0	886/14	783/117	834/66
	5	900/0	900/0	900/0	900/0	900/0	900/0	900/0	900/0	900/0	900/0
	6	900/0	900/0	900/0	900/0	900/0	900/0	900/0	900/0	900/0	900/0
Foobot Home	4	870/30	870/30	870/30	870/30	870/30	870/30	870/30	840/60	870/30	870/30
	5	897/3	900/0	900/0	900/0	896/4	900/0	900/0	870/30	866/34	900/0
	6	893/7	900/0	900/0	900/0	900/0	900/0	900/0	868/32	894/6	900/0
Nanoleaf Shapes	4	857/43	794/106	894/6	440/460	893/7	900/0	752/148	897/3	845/55	712/188
	5	829/71	879/21	893/7	483/417	871/29	881/19	793/107	895/5	881/19	785/115
	6	850/50	891/9	885/15	862/38	878/22	900/0	885/15	899/1	851/49	713/187
<b>Number Correct Accuracy</b>	/48	48	48	48	47	48	48	48	48	48	48
		100.00%	100.00%	100.00%	97.92%	100.00%	100.00%	100.00%	100.00%	100.00%	100.00%
	/41408	40569	40824	41023	40009	40908	40928	40841	40960	40674	40482
<b>Number Correct Accuracy</b>		97.97%	98.59%	99.07%	96.62%	98.79%	98.84%	98.63%	98.92%	98.23%	97.76%

Table 9. Mean similarity scores for each of the 10 runs over each of the four days per device.

Device	Day	R1	R2	R3	R4	R5	R6	R7	R8	R9	R10
Cisco SG200	4	0.0016	0.0011	0.0022	0.0002	0.0010	0.0000	0.0003	0.0001	0.0020	0.0037
	5	0.0009	0.0006	0.0012	0.0001	0.0005	0.0000	0.0002	0.0001	0.0011	0.0020
	6	0.0009	0.0006	0.0013	0.0001	0.0005	0.0000	0.0002	0.0001	0.0011	0.0021
Cisco WAP321	4	0.0021	0.0045	0.0036	0.0003	0.0036	0.0001	0.0052	0.0003	0.0041	0.0028
	5	0.0017	0.0029	0.0027	0.0002	0.0024	0.0001	0.0013	0.0002	0.0031	0.0015
	6	0.0462	0.0378	0.0240	0.0382	0.0181	0.0568	0.0045	0.0058	0.0189	0.0311
Dyson Fan	4	0.0052	0.0018	0.0027	0.0004	0.0065	0.0000	0.0002	0.0001	0.0009	0.0004
	5	0.0046	0.0040	0.0038	0.0007	0.0076	0.0000	0.0003	0.0003	0.0022	0.0009
	6	0.0100	0.0072	0.0045	0.0005	0.0107	0.0009	0.0002	0.0003	0.0044	0.0013
LIFX A19	4	0.0002	0.0110	0.0004	0.0333	0.0002	0.0000	0.0114	0.0000	0.0002	0.0003
	5	0.0630	0.0003	0.0300	0.0000	0.0491	0.0150	0.0000	0.0000	0.0396	0.0257
	6	0.0589	0.0003	0.0647	0.0000	0.0358	0.0166	0.0000	0.0001	0.0565	0.0178
MeRoss-425	4	0.0410	0.0159	0.0484	0.0234	0.0648	0.0372	0.0011	0.0349	0.0349	0.0391
	5	0.0342	0.0734	0.0259	0.0773	0.0520	0.0295	0.0679	0.0041	0.0074	0.0152
	6	0.0766	0.1204	0.0836	0.1789	0.1038	0.0789	0.1185	0.0976	0.0640	0.0671
MeRoss-420	4	0.0286	0.0690	0.0283	0.0160	0.0481	0.0029	0.0058	0.0084	0.0277	0.0183
	5	0.0374	0.1003	0.0211	0.0482	0.0606	0.0060	0.0183	0.0062	0.0650	0.0446
	6	0.0422	0.0752	0.0369	0.0186	0.0789	0.0013	0.0014	0.0103	0.0626	0.0527
Tapo L530e	4	0.0023	0.0055	0.0018	0.0001	0.0040	0.0001	0.0002	0.0001	0.0026	0.0007
	5	0.0063	0.0090	0.0025	0.0009	0.0057	0.0005	0.0003	0.0003	0.0051	0.0009
	6	0.0427	0.0196	0.0114	0.0205	0.0078	0.0063	0.0209	0.0238	0.0185	0.0323
TPLink HS110	4	0.0074	0.0056	0.0051	0.0011	0.0045	0.0000	0.0001	0.0000	0.0038	0.0017
	5	0.0087	0.0047	0.0066	0.0008	0.0060	0.0000	0.0008	0.0002	0.0099	0.0033
	6	0.0089	0.0078	0.0046	0.0032	0.0066	0.0000	0.0008	0.0003	0.0156	0.0039
Hoze	4	0.0086	0.0008	0.0007	0.0002	0.0003	0.0000	0.0000	0.0000	0.0002	0.0005
	5	0.0093	0.0020	0.0015	0.0002	0.0011	0.0010	0.0001	0.0000	0.0035	0.0009
	6	0.0205	0.0116	0.0036	0.0003	0.0009	0.0007	0.0008	0.0002	0.0022	0.0021
Energenie	4	0.0671	0.0041	0.0226	0.0497	0.0384	0.0097	0.0008	0.0321	0.1029	0.0780
	5	0.0006	0.0008	0.0007	0.0001	0.0006	0.0000	0.0000	0.0001	0.0004	0.0003
	6	0.0021	0.0023	0.0027	0.0002	0.0025	0.0000	0.0000	0.0002	0.0012	0.0009
Foobot Home	4	0.0448	0.0392	0.0382	0.0333	0.0400	0.0336	0.0341	0.0692	0.0446	0.0359
	5	0.0202	0.0113	0.0057	0.0007	0.0267	0.0002	0.0080	0.0329	0.0386	0.0038
	6	0.0318	0.0091	0.0051	0.0006	0.0168	0.0004	0.0021	0.0352	0.0171	0.0042
Nanoleaf Shapes	4	0.0020	0.0003	0.0002	0.0000	0.0001	0.0000	0.0000	0.0000	0.0001	0.0000
	5	0.1042	0.1675	0.0375	0.5187	0.0522	0.0040	0.1826	0.0179	0.0953	0.2014
	6	0.1361	0.0727	0.0428	0.4552	0.0737	0.0232	0.1446	0.0197	0.0534	0.1392
<b>Number Correct</b>	4	48	48	48	47	48	48	48	48	48	48
	5	100.00%	100.00%	100.00%	97.92%	100.00%	100.00%	100.00%	100.00%	100.00%	100.00%
	6	0.0289	0.0179	0.0212	0.0318	0.0160	0.0083	0.0170	0.0094	0.0047	0.0139

Table 10. Hedges' g scores for each of the 10 runs over each of the four days per device.

Device	Day	R1	R2	R3	R4	R5	R6	R7	R8	R9	R10
Cisco SG200	4	0.1213	0.1426	0.1332	0.1465	0.1386	0.1271	0.0909	0.1044	0.1325	0.1229
	5	0.0000	0.0000	0.0000	0.0000	0.0000	0.0000	0.0000	0.0000	0.0000	0.0000
	6	0.0069	0.0016	0.0055	0.0015	0.0026	0.0051	0.0102	0.0100	0.0047	0.0071
	7	0.0279	0.0459	0.0385	0.0016	0.0188	0.0105	0.0143	0.0558	0.0206	0.0123
Cisco WAP321	4	0.1168	0.1546	0.1013	0.1393	0.1296	0.0472	0.1506	0.1288	0.0873	0.1435
	5	0.0000	0.0000	0.0000	0.0000	0.0000	0.0000	0.0000	0.0000	0.0000	0.0000
	6	0.3495	0.3293	0.2755	0.3190	0.2683	0.3575	0.1065	0.2407	0.2435	0.3140
	7	0.3240	0.3159	0.2425	0.2824	0.2377	0.3512	0.0605	0.2229	0.2091	0.3012
Dyson Fan	4	0.0324	-0.2519	-0.1042	-0.1076	-0.0561	0.0574	-0.0710	-0.1338	-0.2617	-0.1502
	5	0.0000	0.0000	0.0000	0.0000	0.0000	0.0000	0.0000	0.0000	0.0000	0.0000
	6	0.1691	0.2000	0.0512	-0.0730	0.1178	0.0653	-0.0623	-0.0025	0.1437	0.1052
	7	0.2485	0.2370	0.2352	0.2587	0.2323	0.2448	0.2582	0.2566	0.2430	0.2502
LIFX A19	4	-0.2436	0.2404	0.0383	0.2624	-0.3372	0.0412	0.2180	0.1333	-0.0368	0.1458
	5	0.4551	-0.0108	0.4470	-0.0755	0.4475	0.2946	0.0155	0.1957	0.4400	0.3633
	6	0.4384	0.0502	0.4316	-0.0987	0.4542	0.3224	0.0111	0.1699	0.4466	0.3300
	7	-0.0849	0.0439	-0.0107	-0.0664	-0.3559	0.1320	0.0214	0.1694	0.0794	0.0664
MeRoss-425	4	0.0191	-0.1676	0.0962	0.1556	0.1052	0.0854	0.0846	0.2482	0.1616	0.2041
	5	-0.0222	0.2051	-0.1071	0.3417	0.0206	0.0377	0.3867	0.0661	-0.1462	0.0654
	6	0.1954	0.3915	0.2680	0.6406	0.2960	0.2842	0.5520	0.4625	0.3048	0.3368
	7	0.4039	-0.2292	0.4784	-0.4739	0.5193	0.5242	-0.3159	0.5913	0.4559	0.5331
MeRoss-420	4	0.2551	0.1105	0.2099	0.0877	0.0650	0.1297	0.3504	0.1745	-0.0297	0.0144
	5	0.3201	0.2712	0.1385	0.2940	0.1966	0.2423	0.3176	0.1044	0.2583	0.4510
	6	0.3839	0.1388	0.3317	0.1054	0.3065	0.0949	0.4199	0.1860	0.2332	0.4420
	7	0.3089	0.0288	0.1999	0.1965	0.1249	0.1733	0.3199	-0.0195	0.1427	0.0951
Tapo L530e	4	-0.1079	-0.1897	-0.2050	-0.1617	-0.0895	0.0617	-0.1118	-0.1646	-0.1680	-0.1634
	5	0.2472	-0.1027	-0.1337	0.1113	0.0146	0.1605	-0.0201	-0.0018	-0.0057	-0.1521
	6	0.3349	0.1131	0.2693	0.2505	0.1214	0.2485	0.2433	0.2454	0.2721	0.2566
	7	-0.0123	-0.1769	-0.1950	-0.1406	-0.0616	0.0779	-0.1198	-0.1632	-0.1010	-0.1668
TPLink HS110	4	0.1719	0.2582	0.1297	0.0941	0.0903	0.0731	-0.0878	-0.0645	0.0065	0.1144
	5	0.3079	0.3348	0.2714	0.0362	0.2236	0.1226	0.1563	0.0900	0.2551	0.3239
	6	0.2732	0.2542	0.1375	0.1643	0.2133	0.1439	0.1286	0.0786	0.3070	0.2498
	7	0.3445	0.4968	0.3582	0.2605	0.3907	0.1040	0.2911	0.1219	0.3881	0.2980
Hoze	4	-0.0356	-0.2651	-0.2603	-0.0292	-0.2962	-0.2869	-0.2653	-0.0415	-0.2963	-0.1853
	5	0.0028	0.0089	0.0021	-0.0112	-0.0035	0.0030	0.0336	0.0218	0.0074	-0.0031
	6	0.3095	0.3323	0.2734	0.1010	-0.0656	-0.0536	0.3241	0.3263	-0.0995	0.2813
	7	0.0362	0.0236	0.0040	-0.0419	-0.0064	-0.0186	0.0760	-0.0031	0.0008	-0.0335
Energenie	4	0.5345	0.3356	0.5447	0.4875	0.5368	0.2215	0.4973	0.3500	0.5665	0.5321
	5	-0.0767	-0.0615	-0.1410	0.1051	-0.1334	0.0556	-0.0057	0.0780	-0.0354	-0.0635
	6	0.8335	0.7543	0.7842	0.5325	0.9863	0.7294	1.1153	0.6369	0.9500	0.8050
	7	-0.3732	-0.2461	-0.3173	-0.1263	-0.4101	-0.2454	-0.3534	-0.2240	-0.3334	-0.3373
Foobot Home	4	0.3499	0.3085	0.3009	0.2628	0.3158	0.2649	0.2685	0.4231	0.3506	0.2833
	5	0.3715	0.4142	0.2973	0.1805	0.3945	0.2922	0.3284	0.2859	0.4247	0.3361
	6	0.4296	0.3545	0.4319	0.2155	0.4390	0.3805	0.2525	0.3836	0.3399	0.4165
	7	0.2383	0.2552	0.2943	0.1725	0.1962	0.3033	0.2501	0.1672	0.4747	0.2062
Nanoleaf Shapes	4	0.7162	0.7970	0.4269	1.6676	0.5865	0.3746	0.7947	0.4211	0.6512	0.8008
	5	0.7936	0.6684	0.4631	1.4745	0.5792	0.2594	0.7274	0.4012	0.5300	0.6786
	6	0.7083	0.1621	0.4512	0.2790	0.6012	0.2780	0.2196	0.5035	0.7232	0.8231
	7	0.1463	0.1205	0.1708	0.2434	0.0915	0.2043	0.2031	0.1808	-0.1191	-0.0784
<b>Number Correct</b>	/48	43	45	46	44	42	46	44	45	43	42
		89.58%	93.75%	95.83%	91.67%	87.50%	95.83%	91.67%	93.75%	89.58%	87.50%

## B EXTENDED VERSION CHANGE RESULTS

Table 11. Mean similarity scores for each of the 10 runs over each of the four days per device.

Device & Version Change	Day	R1	R2	R3	R4	R5	R6	R7	R8	R9	R10
MeRoss-420 v3.1.1 -> v3.2.2	8	0.5150	0.2351	0.2287	0.9341	0.3430	0.9455	0.8837	0.0589	0.5872	0.3567
	9	0.5370	0.2566	0.2513	0.9395	0.3607	0.9260	0.9063	0.0616	0.6082	0.4167
	10	0.5065	0.2550	0.2272	0.9288	0.3575	0.9389	0.9193	0.0588	0.5908	0.4083
MeRoss-425 v4.1.6 -> v4.2.3	8	0.0824	0.0215	0.3828	0.6478	0.0555	0.1333	0.5809	0.0042	0.0310	0.0576
	9	0.9998	0.9918	0.9989	1.0000	0.9960	1.0000	1.0000	0.8277	0.9540	0.9992
	10	0.9999	0.9960	0.9995	1.0000	0.9973	0.9999	1.0000	0.8412	0.9784	0.9995
LIFX A19 v2.7 -> v2.8	8	0.9999	0.9937	0.9986	1.0000	0.9967	0.9998	0.9999	0.8072	0.9379	0.9983
	9	1.0000	1.0000	1.0000	1.0000	1.0000	1.0000	1.0000	0.9996	1.0000	1.0000
	10	0.1644	0.0576	0.0530	0.0845	0.1000	0.0722	0.1393	0.0106	0.1162	0.1455
LIFX A19 v2.7 -> v2.9	8	0.1095	0.0384	0.0516	0.0833	0.0555	0.0474	0.0912	0.0047	0.0523	0.1480
	9	0.0432	0.0317	0.0428	0.0237	0.0296	0.0227	0.0451	0.0042	0.0314	0.1478
	10	0.1116	0.0606	0.0562	0.0519	0.0544	0.0568	0.1055	0.0040	0.0581	0.1709
TPLink HS110 v1.0.10 -> v1.2.6	8	0.2458	0.1605	0.2886	0.5810	0.4664	0.2354	0.7800	0.6090	0.8738	0.9178
	9	0.2761	0.1505	0.2772	0.5149	0.4295	0.3019	0.7388	0.5733	0.8887	0.9271
	10	0.3181	0.1362	0.3437	0.3438	0.2959	0.4061	0.6579	0.6177	0.9134	0.9325
Nanoleaf Shapes v6.5.1 -> v7.1.0	8	0.3653	0.2503	0.3095	0.5242	0.4942	0.3781	0.7573	0.6927	0.9346	0.9459
	9	0.6973	0.9401	0.9442	0.9845	0.8251	0.6512	0.9184	0.8407	0.9789	0.4252
	10	0.6842	0.9373	0.9444	0.9960	0.8291	0.6479	0.9531	0.8424	0.9827	0.4464
Nanoleaf Shapes v6.5.1 -> v7.1.1	8	0.7128	0.9396	0.9427	0.9954	0.8285	0.7546	0.9599	0.8486	0.9821	0.4847
	9	0.9609	0.9685	0.9744	0.9565	0.9487	0.9985	0.9975	0.9962	0.9899	0.9669
	10	0.0338	0.0407	0.0541	0.0635	0.0432	0.0035	0.0063	0.0187	0.0399	0.0507
Tapo L530e v1.2.2->v1.2.4	8	0.0537	0.0582	0.0529	0.0663	0.0323	0.0229	0.0138	0.0068	0.0367	0.0630
	9	0.0400	0.0384	0.0484	0.0604	0.0471	0.0041	0.0103	0.0055	0.0382	0.0744
	10	0.0417	0.0286	0.0506	0.0439	0.0310	0.0026	0.0079	0.0087	0.0242	0.0541
Tapo L530e v1.2.2->v1.2.4	8	0.0614	0.0435	0.0407	0.0706	0.0504	0.0064	0.0196	0.0124	0.0415	0.0869
	9	0.1057	0.0559	0.0802	0.0677	0.1218	0.0014	0.0246	0.0668	0.0487	0.1029
	10	0.1476	0.0928	0.0751	0.1968	0.1734	0.0380	0.0656	0.0717	0.1084	0.1548
Number Correct Accuracy	/32	11	8	8	15	8	11	16	12	15	9
		34.38%	25.00%	25.00%	46.88%	25.00%	34.38%	50.00%	37.50%	46.88%	28.13%

Table 12. Hedges' g scores for each of the 10 runs over each of the four days per device.

Device & Version Change	Day	R1	R2	R3	R4	R5	R6	R7	R8	R9	R10
MeRoss-420 v3.1.1 -> v3.2.2	8	2.1028	1.1035	1.6839	9.3189	1.8878	12.4747	5.9543	1.0708	3.0107	1.7330
	9	2.1469	1.1780	1.7098	9.5425	1.8562	8.8756	6.8428	1.0994	3.2415	1.7513
	10	1.9494	1.1882	1.6788	8.6755	1.9488	10.3359	7.6433	1.0532	3.1604	1.7564
MeRoss-425 v4.1.6 -> v4.2.3	8	0.9797	-0.3105	1.7521	3.3667	1.1403	0.8024	1.9730	0.0684	0.0091	0.6358
	9	7.7575	9.5076	13.1812	48.9108	13.9206	13.2780	460.2742	4.4575	18.3008	41.8124
	10	7.7583	9.5678	13.1899	48.9107	13.9471	13.2762	460.2726	4.8761	21.8902	41.8282
LIFX A19 v2.7 -> v2.8	8	7.7579	9.5384	13.1765	48.9107	13.9377	13.2746	453.7518	3.8652	9.9640	41.5527
	9	7.7591	9.6208	13.1966	48.9108	14.0034	13.2780	460.2750	192.2422	23.5844	41.8549
	10	0.6671	0.7018	0.8931	0.6090	0.6646	0.5317	0.7489	0.4198	0.6978	0.9352
LIFX A19 v2.7 -> v2.9	8	0.5573	0.8615	1.1473	0.5349	0.5644	0.5137	0.6266	1.0812	0.5126	1.1882
	9	0.3623	1.1259	1.2871	0.4729	0.5250	0.3970	0.5294	1.2820	0.3913	1.1817
	10	0.5436	0.7963	1.1658	0.5872	0.6006	0.5238	0.6538	1.0069	0.5630	1.2840
TPLink HS110 v1.0.10 -> v1.2.6	8	1.7139	2.1214	2.4255	3.0095	2.8912	1.5894	8.2776	3.7322	8.3592	16.8919
	9	1.7422	1.7386	2.2693	2.9228	2.7974	1.8566	6.8519	3.4600	18.0185	17.4591
	10	1.9929	1.5404	2.3630	2.0136	2.0116	2.1438	6.0980	4.1212	22.3034	21.8738
Nanoleaf Shapes v6.5.1 -> v7.1.0	8	1.7423	1.9442	2.1459	2.4219	2.6928	1.9058	6.5724	4.5947	22.3749	24.3228
	9	3.7166	9.4490	10.8561	22.4223	3.4429	2.8883	5.7269	3.6479	22.1229	2.5343
	10	3.3689	9.4888	11.5650	66.7936	3.5080	2.9832	10.6339	3.6990	24.6844	2.9129
Nanoleaf Shapes v6.5.1 -> v7.1.1	8	3.8026	9.9704	11.0020	61.6774	3.4657	4.0308	12.4393	3.8333	23.6409	3.5436
	9	24.7653	17.2634	22.1398	10.9875	12.1878	68.3644	158.4885	85.6187	26.4892	34.7168
	10	0.2130	0.3348	0.7031	0.5125	0.4199	0.3212	0.1637	0.2482	0.6411	0.3284
Tapo L530e v1.2.2->v1.2.4	8	0.3101	0.4518	0.4698	0.5114	0.4180	0.3113	0.2234	0.2594	0.6479	0.3838
	9	0.2517	0.3885	0.6482	0.5141	0.5054	0.2740	0.2069	0.2495	0.7047	0.4533
	10	0.3101	0.3066	0.5527	0.4241	0.3592	0.2450	0.1704	0.2754	0.5049	0.3513
Number Correct Accuracy	/32	22	21	27	24	24	20	21	20	26	23
		68.75%	65.63%	84.38%	75.00%	75.00%	62.50%	65.63%	62.50%	81.25%	71.88%

Table 13. Number of samples that are below (left of bracket) and above (right of bracket) the 0.5 threshold for each of the 10 runs over each of the four days per device.

Device & Version Change	Day	R1	R2	R3	R4	R5	R6	R7	R8	R9	R10
MeRoss-420 v3.1.1 -> v3.2.2	8	2.1028	1.1035	1.6839	9.3189	1.8878	12.4747	5.9543	1.0708	3.0107	1.7330
	9	2.1469	1.1780	1.7098	9.5425	1.8562	8.8756	6.8428	1.0994	3.2415	1.7513
	10	1.9494	1.1882	1.6788	8.6755	1.9488	10.3359	7.6433	1.0532	3.1604	1.7564
	11	0.9797	-0.3105	1.7521	3.3667	0.1403	0.8024	1.9750	0.0684	0.0091	0.6358
MeRoss-425 v4.1.6 -> v4.2.3	8	7.7575	9.5076	13.1812	48.9108	13.9206	13.2780	460.2742	4.4575	18.3008	41.8124
	9	7.7583	9.5678	13.1899	48.9107	13.9471	13.2762	460.2726	4.8761	21.8902	41.8282
	10	7.7579	9.5384	13.1765	48.9107	13.9377	13.2746	453.7518	3.8652	9.9640	41.5527
	11	7.7591	9.6208	13.1966	48.9108	14.0034	13.2780	460.2750	192.2422	23.5844	41.8549
LIFX A19 v2.7 -> v2.8	8	0.6671	0.7018	0.8931	0.6090	0.6646	0.5317	0.7489	0.4198	0.6978	0.9352
	9	0.5573	0.8615	1.1473	0.5349	0.5644	0.5137	0.6266	1.0812	0.5126	1.1882
	10	0.3623	1.1259	1.2871	0.4729	0.5250	0.3970	0.5294	1.2820	0.3913	1.1817
	11	0.5436	0.7963	1.1658	0.5872	0.6006	0.5238	0.6538	1.0069	0.5630	1.2840
LIFX A19 v2.7 -> v2.9	8	1.7139	2.1214	2.4255	3.0095	2.8912	1.5894	8.2776	3.7322	8.3592	16.8919
	9	1.7422	1.7386	2.2693	2.9228	2.7974	1.8566	6.8519	3.4600	18.0185	17.4591
	10	1.9929	1.5404	2.3630	2.0136	2.0116	2.1438	6.0980	4.1212	22.3034	21.8738
	11	1.7423	1.9442	2.1459	2.4219	2.6928	1.9058	6.5724	4.5947	22.3749	24.3228
TPLink HS110 v1.0.10 -> v1.2.6	8	3.7166	9.4490	10.8561	22.4223	3.4429	2.8883	5.7269	3.6479	22.1229	2.5343
	9	3.3689	9.4888	11.5650	66.7936	3.5080	2.9832	10.6339	3.6990	24.6844	2.9129
	10	3.8026	9.9704	11.0020	61.6774	3.4657	4.0308	12.4393	3.8333	23.6409	3.5436
	11	24.7653	17.2634	22.1398	10.9875	12.1878	68.3644	158.4885	85.6187	26.4892	34.7168
Nanoleaf Shapes v6.5.1 -> v7.1.0	8	0.2130	0.3348	0.7031	0.5125	0.4199	0.3212	0.1637	0.2482	0.6411	0.3284
	9	0.3101	0.4518	0.4698	0.5114	0.4180	0.3113	0.2234	0.2594	0.6479	0.3838
	10	0.2517	0.3885	0.6482	0.5141	0.5054	0.2740	0.2069	0.2495	0.7047	0.4533
	11	0.3101	0.3066	0.5527	0.4241	0.3592	0.2450	0.1704	0.2754	0.5049	0.3513
Nanoleaf Shapes v6.5.1 -> v7.1.1	8	0.3950	0.4281	0.5751	0.4513	0.5319	0.2074	0.2978	0.3034	0.6555	0.4899
	9	0.6526	0.4084	0.6985	0.4639	0.8097	0.2606	0.4111	0.4524	0.6581	0.6171
	10	0.8118	0.5859	0.6231	0.8375	0.8613	0.3219	0.4449	0.5088	0.6662	0.7253
	11	1.0121	0.5434	0.8166	1.0436	0.9575	0.5645	0.5213	0.5319	0.7397	0.7976
Tapo L530e v1.2.2->v1.2.4	8	0.1391	-0.1601	-0.1440	-0.0189	-0.0478	0.1402	0.0171	0.0054	-0.1251	-0.1522
	9	0.1515	-0.0584	-0.0423	0.0761	-0.0315	-0.0071	0.1178	0.1086	-0.0613	0.0199
	10	0.1562	-0.1303	-0.0833	-0.0754	-0.0588	0.1076	-0.0073	-0.1025	0.0180	-0.1399
	11	0.0089	-0.0299	-0.0737	0.0865	-0.0560	0.0734	-0.0124	0.0450	-0.0668	-0.0277
Number Correct	/32	22	21	27	24	24	20	21	20	26	23
Accuracy		68.75%	65.63%	84.38%	75.00%	75.00%	62.50%	65.63%	62.50%	81.25%	71.88%

Received 10 July 2024